Scanning Electron Microscope (SEM) Instrumentation

J. Goldstein et al., *Scanning Electron Microscopy and X-Ray Microanalysis*,
https://doi.org/10.1007/978-1-4939-6676-9_5

5.1 Electron Beam Parameters

This chapter addresses essential topics: the quantitative attributes of an electron beam, well-known widely-used SEM modes, and electron detectors.

Why Learn About Electron Optical Parameters?

As we mentioned in the introduction to the book, the main goal of the text is to help users understand how to operate the SEM and its accessories, and how to be effective at using these powerful tools for materials characterization and analysis. It is a fair question, then, to ask why an operator of the microscope needs to understand electron optics and the optical parameters of the beam. Clearly an SEM design engineer needs to be conversant in these subjects, but why learn these concepts as an end user? The simplest answer is that while all SEMs have knobs, switches, and controls, in the end it is the electron optical beam parameters that the operator is controlling, and a basic understanding of what is being changed by those knobs is essential to becoming a skilled user. Whether the knobs and dials are "old-school" analog hardware devices or purely virtual objects that exist only in a software user interface, the operator cannot use the SEM to best advantage without a clear picture of how those knobs are changing the beam.

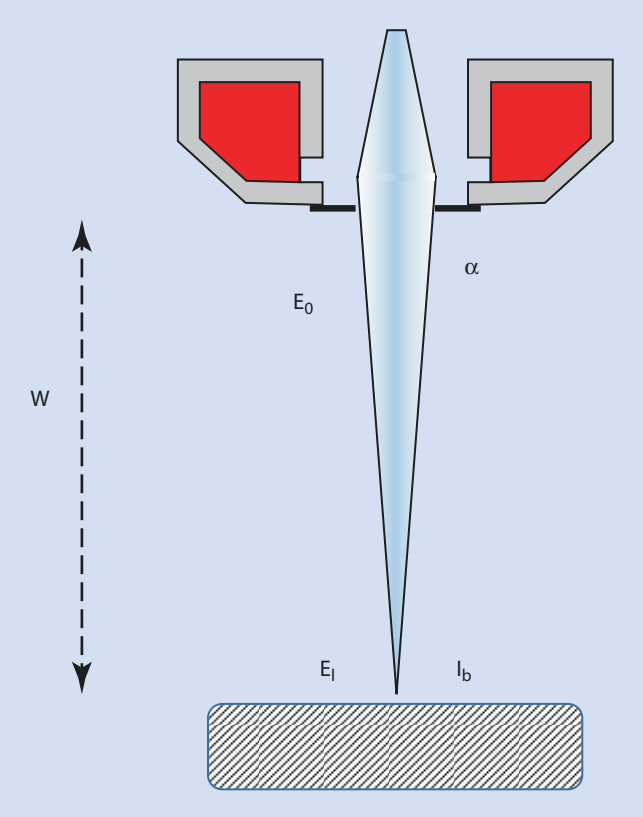

Fig. 5.1 Basic elements of the electron beam in an SEM

5.2 Electron Optical Parameters

Figure 5.1 shows the basic features of an electron beam in a scanning electron microscope after it emerges from the final aperture of the objective lens and before it impacts the sample surface. While changes to the beam inside the electron gun and inside the electron column are also important to the SEM operator, a thorough understanding of the attributes of the beam in the chamber is absolutely essential to mastery of the instrument.

5.2.1 Beam Energy

One of the fundamental beam parameters is the energy of the electrons in the beam, measured in electronvolts (eV) and often represented by the symbol E, or E_0. This parameter represents the *initial* energy of the electrons as they enter the SEM chamber or the sample. Beam energy has a direct effect on many important aspects of SEM operation, such as the size of the excitation volume in the sample and the intensity of the X-rays emitted, so it is necessary to choose this parameter carefully and set it to an appropriate value before acquiring data. Frequently the beam energy is several thousand electronvolts or higher, so the kilo-electronvolt is the most common unit of beam energy, abbreviated keV. One keV is equal to 1000 eV, and many SEMs are capable of generating electron beams up to 30 keV (equal to 30,000 eV), or in a few cases even higher.

If you have any experience with electronics or electrical engineering, the electronvolt as a unit of energy may be confusing at first since it sounds more like a measure of voltage, unlike the more common units of energy such as the Joule, the calorie, or the erg. The terms *electron volt* and the related SI unit *electronvolt* are related to the method used by the SEM to impart energy to the electrons that emerge from the electron source. Typically, the electrons are accelerated from low energy to high energy using an electrostatic potential difference generated by a high-voltage power supply. Negatively charged electrons are repelled from surfaces with negative electrical potential and attracted to surfaces with positive potential, and the potential difference is measured in volts. One electronvolt is simply the energy acquired by an electron when it is accelerated through a potential difference of one volt; similarly, an electron that drops through a voltage difference of 20 kilovolts (20 kV) emerges with an energy of 20 keV.

This underlying connection between the accelerating voltage used by the microscope and the resulting beam energy can help make sense of the different terminology often used in the SEM community regarding "beam energy." On many microscopes, you set the accelerating voltage with a knob or by using a graphical user interface on a computer. On these microscopes, you would select 30 kV for the accelerating voltage if you wanted to work at high beam energy, or you might select 1 kV if you wished to work at low voltage. Other microscope interfaces allow you to select the beam energy directly instead of the accelerat-

ing voltage, so the corresponding settings would be 30 keV for high beam energy work and 1 keV for low-voltage operation. In informal conversation it is common to hear 30 kV and 30 keV used interchangeably to mean the same beam setting, and usually no confusion arises from this practice. However, in written documents such as reports of analyses or academic publications, the common error of describing the beam energy using units of kilovolts or of recording the accelerating voltage in units of kilo-electronvolts should be avoided.

Landing Energy

Aside from this possible confusion between beam energy and accelerating potential, there are other subtleties in the proper characterization of the beam energy in the SEM. Depending on the technology used by the microscope manufacturer, the electrons in the microscope may change energy more than once during their path from the electron source to the surface of the sample. Some microscopes seek to improve imaging performance by modifying the electrons' energy during the mid-portion of the optical column. On more recent microscope models it is increasingly common to see beam deceleration options, which decrease the beam energy just before the electrons emerge from the objective lens.

Also common on modern instruments is the option to apply a voltage bias to the sample itself, thus allowing the SEM operator to increase the energy of the electrons as they approach the sample (in the case of a positive sample bias), or decrease the energy of the electrons (in the case of a negative sample bias). For example, if the electron beam emerges from the objective lens into the SEM sample chamber with a beam energy of 5 keV, but the sample has a negative voltage bias of 1 kV applied, the electrons will be decelerated to an energy of 4 keV when they impact the specimen.

The term used to describe the electron beam energy at the point of impact on the sample surface is *landing energy*, usually denoted by the symbol E_l. The physics of beam–specimen interaction depends only on the landing energy of the electrons, not on their energy at points further up the optical path. Critically important phenomena such as the size of the excitation volume in the specimen, the number of characteristic X-ray peaks available for use in compositional measurements, or the high energy limit of continuum X-rays emitted (the Duane–Hunt limit) are all functions of the landing energy, not the initial beam energy. Because of this, it is very important for the SEM operator to understand when landing energy differs from the beam energy at the objective lens final aperture, and how to control the value of the landing energy. The details of such subtleties vary from one vendor to another, and even from one microscope model to the next, but they are invariably described in the user documentation for every instrument. Seek help from your microscope's customer support team or an application engineer if you are not absolutely clear on how to control the landing energy on your microscope. In many situations, particularly when working with older microscopes, this distinction is not important and the terms *beam energy* and *landing energy* may be used interchangeably without a problem, but when the distinction matters it can be crucial to accurate analysis and proper communication or reporting.

5.2.2 Beam Diameter

Another important electron beam characteristic under the control of the SEM operator is the diameter of the electron beam, which in most cases refers to the diameter of the beam as it impacts the sample surface. Beam diameter has units of length and is frequently measured in nanometers, Ångstroms, or micrometers, depending on the size of the beam. For most SEM applications the beam diameter will fall within the broad range of 1 nm to 1 µm. It is commonly represented by the symbol d, or a subscripted variant such as d_{probe} or d_p.

Before developing an understanding of the importance of beam–specimen interactions, many SEM operators naively assume that the resolution of their SEM images is dictated solely by the beam diameter. While this may be true in some situations, more often the relationship between the beam diameter and the resolution is a complex one. Perhaps this explains why the exact definition of beam diameter is not always provided, even in relatively careful writing or formal contexts. The simplest model of an electron beam is one where the beam has a circular cross section at all times, and that the electrons are distributed with uniform intensity everywhere inside the beam diameter and are completely absent outside the beam diameter. In this trivial case, the beam has hard boundaries and is the same size no matter which azimuth you use to measure it. In reality the electron beam in an SEM is much more complicated. Even if you assume that the cross section is circular, electron beams exhibit a gradient of electron density from the core of the beam out to the edges, and in many cases have a tail of faint intensity that extends quite far from the central flux. It is still possible in these case to define the meaning of beam diameter in a precise way, in terms of the full width at half-maximum of the intensity for example, or the full width at tenth-maximum if the tails are pronounced. More careful statistical models of the beam will specify the radial intensity distribution function—a Gaussian or Lorentzian distribution, for example—and will allow for non-circularity. In most situations where such precision is not warranted, however, it will suffice to assume that the beam diameter is a single number that characterizes the width in nanometers of that portion of the beam that gives rise to the most important fraction of the contrast or sample excitation as measured at the surface of the specimen.

5.2.3 Beam Current

Of all the electron beam parameters that matter to the SEM operator, beam current is perhaps highest on the list. Fortunately it is a relatively simple parameter to understand since it is entirely analogous to electrical currents of the kind

found in wires, electronics, or electrical engineering. Beam current at the sample surface is a measure of the number of electrons per second that impact the specimen. It is usually measured in fractions of an ampere, such as microamperes (μA), nanoamperes (nA), or picoamperes (pA). A typical SEM beam current is about 1 nA, which corresponds to 6.25 × 10^9 electrons per second, or approximately one electron striking the sample every 160 ps . The usual symbol used to represent beam current is *I*, or *i*, or a subscripted variant such as I_{probe}, I_{beam}, I_p, or I_b.

5.2.4 Beam Current Density

Similar to the beam current, the concept of current density is relatively easy to understand and corresponds directly with the same concept in electrical engineering or electrical design. Current density in an electron beam is defined as the beam current per unit area, and it is usually represented by the symbol *J*, or J_{beam}. In standard units this quantity is expressed in A/m^2, but there are also derived units better suited to the SEM such as nA/nm^2 or similar. The most important thing to understand about current density is that it is an *areal* measure, not an absolute measure; this means the current depends directly on and varies linearly with the area of the region through which the stated current density passes.

To make this concrete, let's consider an example calculation of the current density in an electron beam. Figure 5.2 shows a circular beam with a diameter of 5 nm; and the total current inside the circular beam spot is 1 nA. The area of the beam is

$$A_{circle} = \pi r^2 = \pi\left(\frac{d}{2}\right)^2 = \pi\left(\frac{5\,nm}{2}\right)^2 = 19.6\,nm^2 \quad (5.1)$$

and therefore the current density in the round beam is

$$J_{circle} = \frac{I_{circle}}{A_{circle}} = \frac{1\,nA}{19.6\,nm^2} = 0.0509\,\frac{nA}{nm^2} = 50.9\,pA/nm^2 \quad (5.2)$$

Figure 5.2b shows the situation if you decrease the diameter of the beam by half, from 5 nm to 2.5 nm, yet keep the same total current in the beam. Now the area has gotten smaller, yet the current is unchanged, so the current density has increased. The new current density is

$$J_{circle} = \frac{I_{circle}}{A_{circle}} = \frac{1\,nA}{4.91\,nm^2} = 0.204\,\frac{nA}{nm^2} = 204\,pA/nm^2 \quad (5.3)$$

Since focusing the electron beam in an SEM changes the diameter of the beam but does not change the beam current, the current density must change. As can be seen in Fig. 5.2, shrinking the beam width by a factor of two results in a four-fold increase in beam current density.

5.2.5 Beam Convergence Angle, α

One of the fundamental characteristics of the electron beam found in all SEM instruments is that the shape of the beam as seen from the side is not a parallel-sided cylinder like a pencil, but rather a cone. The beam is wide where it exits the final aperture of the objective lens, and narrows steadily until (if the sample is in focus) it converges to a very small spot when it enters the specimen. A schematic of this cone is shown in Fig. 5.3. The point where the beam lands on the sample is denoted *S* at the bottom of the cone, and the beam-defining aperture is shown in perspective as a circle at the top of the cone, with line segment *AB* equal to the diameter of that aperture, d_{apt}. The vertical dashed line represents the optical axis of the SEM column, which ideally passes through the center of the final aperture, is perpendicular to the plane of that aperture, and extends down through the chamber into the sample and beyond. The sides of the cone are defined by the "edge" of the electron beam. As mentioned above in the definition of the beam diameter, this notion of a hard-edged

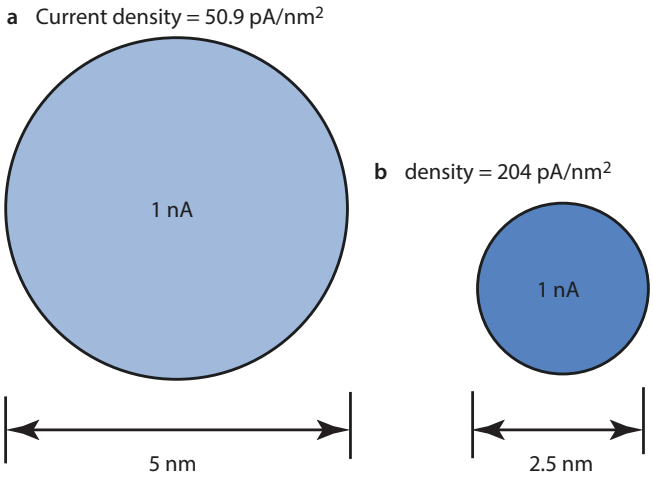

Fig 5.2 **a** Current density in a circular electron beam; **b** current density if the beam diameter is reduced by a factor of two with the same current

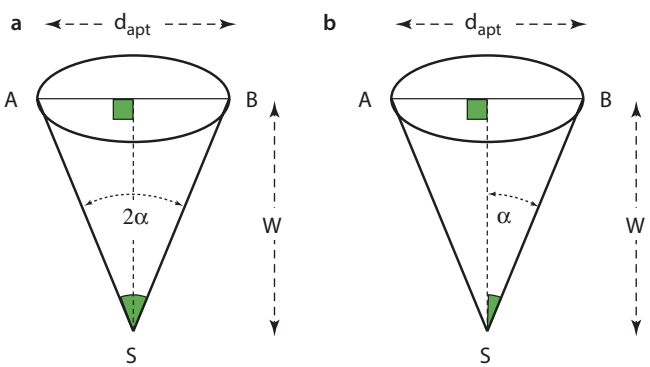

Fig. 5.3 **a** Definition of beam cone opening angle 2α; **b** definition of beam convergence (half) angle α

beam may not be physically realistic, but it is simple to understand and works well for our purposes here of understanding basic beam parameters.

In geometry, the opening angle of a cone is defined as the vertex angle *ASB* at the point of the cone, as shown in Fig. 5.3a. When working with the electron optics of an SEM, by convention we use the term *convergence angle* to describe how quickly the electron beam narrows to its focus as it travels down the optic axis. This convergence angle is shown in Fig. 5.3b as α, which is half of the cone opening angle. In some cases, the beam convergence angle is referred to as the *convergence half-angle* to emphasize that only half of the opening angle is intended.

Generally the numerical value of the beam convergence angle in the SEM is quite small, and the electron beam cones are much sharper and narrower than the cones used for schematic purposes in Fig. 5.3. In fact, if you ground down and reshaped the sides of a sewing needle so that it was a true cone instead of a cylinder sharpened only at the tip, you would then have a cone whose size and shape is reasonably close to the dimensions found in the SEM.

Estimating the value of the convergence angle of an electron beam is not difficult using the triangles drawn in Fig. 5.3. The length of the vertical dashed line along the optical axis is called the *working distance*, usually denoted by the symbol *W*. It is merely the distance from the bottom of the objective lens pole piece (taken here to be approximately the same plane as the final aperture) to the point at which the beam converges, which is typically also the surface of the sample if the sample is in focus. In practical SEM configurations this distance can be as small as a fraction of a millimeter or as large as tens of millimeters or a few centimeters, but in most situations *W* will be between 1 mm and 5 mm or so. The diameter of the wide end of the cone, line segment *AB*, is the aperture diameter, d_{apt}. This can also vary widely depending on the SEM model and the choices made by the operator, but it is certainly no larger than a fraction of a millimeter and can be much smaller, on the order of micrometers. For purposes of concreteness, let's assume *W* is 5 mm (i.e., 5000 μm) and the aperture is 50 μm in diameter (25 μm in radius, denoted r_{apt}).

From Fig. 5.3b we can see that triangle *ASB* is composed of two back-to-back right triangles. The rightmost of these has its vertex angle labeled α. The leg of that triangle adjacent to α is the working distance *W*, the opposite leg is the aperture radius r_{apt}, and the hypotenuse of the right triangle is the slant length of the beam cone, *SB*. From basic trigonometry we know that the tangent of the angle is equal to the length of its opposite leg divided by its adjacent leg, or

$$\tan\alpha = \frac{r_{apt}}{W}, \tag{5.4}$$

$$\alpha = \tan^{-1}\left(\frac{r_{apt}}{W}\right) = \tan^{-1}\left(\frac{25\,\mu\text{m}}{5000\,\mu\text{m}}\right)$$
$$= \tan^{-1}(0.005) = 0.005\,\text{radians} = 5\,\text{mrad}.$$

It is no coincidence that the arc tangent of 0.005 is almost exactly equal to 0.005 radians, since a well-known approximation in trigonometry is that

$$\tan^{-1}\theta = \theta. \tag{5.5}$$

Since in every practical case encountered in SEM imaging the angle will be sufficiently small to justify this approximation, we can write our estimate of the convergence angle in a much simpler form that does not require any trigonometric functions,

$$\alpha = \frac{r_{apt}}{W}, \text{ or } \alpha = \frac{d_{apt}}{2W} \tag{5.6}$$

As mentioned earlier, this angle is quite small, approximately equal to 0.25° or about 17 arc minutes.

5.2.6 Beam Solid Angle

In the previous section we defined the beam convergence angle in terms of 2D geometry and characterized it by a planar angle measured in the dimensionless units of radians. However, the electron beam forms a 3D cone, not a 2D triangle, so in reality it subtends a *solid angle*. This is a concept used in 3D geometry to describe the angular spread of a converging (or diverging) flux. The usual symbol for solid angle is Ω, and its units of measure are called *steradians*, abbreviated *sr*. Usually when solid angles are discussed in the context of the SEM they are used to describe the acceptance angle of an X-ray spectrometer, or sometimes a backscattered electron detector, but they are also important in fully describing the electron optical parameters of the primary beam in the SEM as well as the properties of electron guns.

Figure 5.4 shows the conical electron beam in 3D, emerging from the circular beam-defining aperture at the top

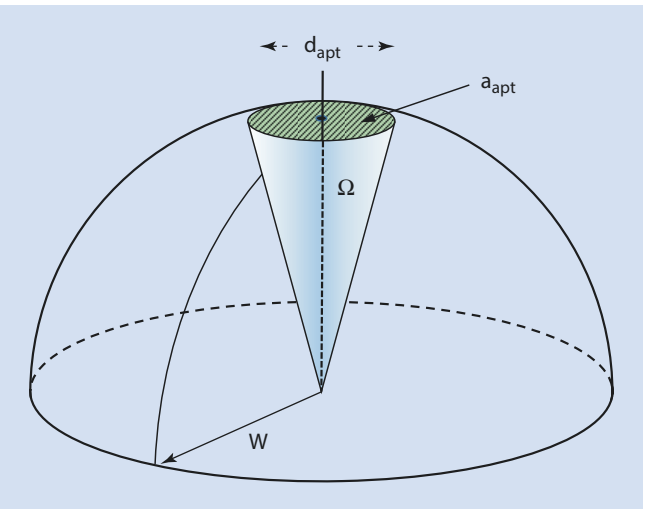

Fig. 5.4 Definition of beam solid angle, Ω. The vertical dashed line represents the optical axis of the SEM, and the distance from the aperture plane to the beam impact point is the working distance, *W*. This is also the radius of the imaginary hemisphere used to visualize the solid angle

of the figure and converging on the sample surface. The diameter of that aperture is d_{apt}, and the area of the aperture is a_{apt}. As discussed earlier, the distance the beam travels vertically from the final aperture to the point where it is focused to a spot is the working distance, W. Now imagine a complete sphere centered on the beam impact point, and with spherical radius equal to W. The upper hemisphere of this imaginary dome is depicted in Fig. 5.4 as well, and since its radius is W, the beam-defining aperture will lie on the surface of this sphere.

5

The key to understanding the meaning of solid angles and their numerical measure using units of steradians is to consider such a complete sphere and the fractional surface area of that sphere that is occupied by the object of interest. Every complete sphere, *regardless of diameter*, subtends exactly 4π steradians of solid angle. It follows that every hemisphere represents a solid angle of 2π steradians, no matter how small or how large the hemisphere might measure in meters. On the other hand, the surface area of a sphere A_{sphere} most certainly depends on the radius r, and can be calculated using the ancient formula

$$A_{sphere} = 4\pi r^2. \tag{5.7}$$

For the imaginary sphere and electron beam aperture shown in Fig. 5.4, we can assume realistic numbers for this calculation by adopting the values used in the beam convergence angle discussion above: $W = 5000$ μm, $d_{apt} = 50$ μm, and $r_{apt} = 25$ μm. With these values we can calculate the surface area of the complete sphere as

$$A_{sphere} = 4\pi W^2 = 4\pi\left(5000\,\mu\text{m}\right)^2 = 3.14\times10^8\,\text{mm}^2. \tag{5.8}$$

and we can calculate the area of the beam-defining aperture as

$$a_{apt} = \pi r_{apt}{}^2 = \pi\left(25\,\mu\text{m}\right)^2 = 1.96\times10^3\,\mu\text{m}^2. \tag{5.9}$$

It is obvious from the diagram that our aperture subtends only a small fraction of the sphere upon which it rests, and it is a simple matter to calculate the value of that fraction,

$$\frac{a_{apt}}{A_{sphere}} = \frac{1.96\times10^3\,\mu\text{m}^2}{3.14\times10^8\,\mu\text{m}^2} = 6.25\times10^{-6}. \tag{5.10}$$

The important step is to realize that if the aperture occupies 6 parts in a million of the whole sphere's surface area, then it must also subtend 6 parts in a million of the 4π steradian solid angle of that whole sphere, so we can calculate the numerical solid angle of the beam by multiplying by this areal fraction

$$\Omega_{beam} = \frac{a_{apt}}{A_{sphere}}\cdot\Omega_{sphere} = \left(6.25\times10^{-6}\right)\cdot\left(4\pi\ \text{steradian}\right) = 7.85\times10^{-5}\ \text{sr}. \tag{5.11}$$

Unless you work with solid angle calculations on a regular basis, this value probably has little physical meaning to you, and you have no sense of how big or how small 78 microsteradians are in real life. To provide some perspective, consider that both the Moon and the Sun subtend about this same solid angle when viewed from the surface of the Earth using the naked eye. The exact angular diameters (and therefore also the solid angles) of both the Sun and the Moon vary slightly during their orbits, depending on how far away they are at any given moment, but this variation is small and oscillates around average values:

$$2\alpha_{Sun} = 9.35\,\text{mrad},\quad \alpha_{Sun} = 4.68\,\text{mrad}$$

$$2\alpha_{Moon} = 9.22\,\text{mrad},\quad \alpha_{Moon} = 4.61\,\text{mrad}$$

$$\Omega_{Sun} = 68.7\,\mu\text{sr}$$

$$\Omega_{Moon} = 66.7\,\mu\text{sr}.$$

Of course the Sun is much, much larger than the Moon in diameter, but it is also much farther away, so the two celestial bodies appear to be about the same angular size from the perspective of the Earthbound viewer. This similarity in angular size is a coincidence, and it is the reason that during a solar eclipse that the Moon almost perfectly occludes the Sun for a short time. This analogy is instructive for the SEM operator because it helps explain how a small final beam aperture combined with a short working distance can produce the same convergence angle (and therefore depth of field) as a configuration that uses a large aperture and a long working distance. Likewise, an energy-dispersive X-ray spectrometer (EDS detector) with a small area of 10 mm^2 can subtend the same solid angle (and therefore collect the same number of X-rays) as a much larger 100-mm^2 detector sitting at a more distant detector-to-sample position.

5.2.7 Electron Optical Brightness, β

In practice the beam solid angle described in the previous section is an obscure and little-used parameter, and it is not that important for most SEM operators to understand fully. However, the concept of beam solid angle and the units of steradians affect the SEM operator much more directly through the concept of electron optical *brightness*, β. The main reason that field emission gun SEMs (FEG SEMs) enjoy drastically improved performance over SEMs that use thermionic tungsten electron sources is because of the much larger electron optical brightness of the FEG electron source. Further, the brightness of the beam when it lands on the sample is the central mathematical variable in one of the key equations of SEM operation, the brightness equation. This equation relates the beam brightness to the beam diameter, the beam current, and the convergence angle, and it is an invaluable tool that lets the SEM operator predict and manage the tradeoff between probe size and beam current.

Because of this central role in practical use of the SEM, it is worth struggling with the mathematics until you understand these concepts and can apply them in your work.

Because the term *brightness* is used in everyday language, most people have an intuitive sense that if one source of energy (say, the Sun) is brighter than another source (say your flashlight or torch) then the brighter source is emitting "more light." In other words, the flux is higher on the receiving end (i.e., at the sensor). Electron optical brightness is similar, but it is more precisely defined, considers current density instead of just total current, and factors in the change in angular divergence of the beam as it is focused or defocused by the electron lenses in the SEM column. Using the terms and concept defined in the sections above, brightness can be succinctly defined as current density per unit solid angle, and it is measured in units of A m^{-2} sr^{-1} (i.e., amperes per square meter per steradian). Based on a quick analysis of the units, it becomes obvious that if two electron beams have exactly the same current and same beam diameter at their tightest focus (and therefore the same current density), but they have different convergence angles, the beam with the smaller convergence angle will have the higher brightness. This is a result of the sr^{-1} term in the units, meaning the solid angle is in the denominator of the definition of brightness, and therefore larger solid angles result in smaller brightnesses (all other things being equal). In the case of visible light, this is why a 1-W laser is far "brighter" than a 200-W light bulb. This simultaneous dependence on current density and angular spread is also the reason for one of the most important properties of brightness as defined above: it is not changed as the electron beam is acted upon by the lenses in the SEM. In other words, to a very good approximation, the brightness of the electron beam is constant as it travels down the SEM from the electron source to the surface of the sample; and if you can estimate its value at one location along the beam you know it everywhere. One variable that does affect the brightness, however, is beam energy. In the SEM the brightness of all electron sources increases linearly with beam energy, and this change must be taken into account if you compare the brightness of beams at different energies.

Brightness Equation

One of the most valuable equations for understanding the behavior of electron beams in the SEM is the brightness equation, which relates the three parameters that define the beam:

$$\beta = \frac{4i}{\pi^2 d^2 \alpha^2} \tag{5.12}$$

If you know the numerical value of the brightness of the beam, measured in A m^{-2} sr^{-1}, then the brightness equation can provide a rough estimate of other parameters such as beam diameter, current, and convergence angle. This can be useful for explaining (quantitatively) the observed performance increase of a FEG SEM over a thermionic instrument, for example. However, even without knowing the numerical value of the brightness β, the functional form of the equation can provide very useful information about changes in the beam.

Because the brightness, even if its value is unknown, is a constant and does not change as you change lens settings from one imaging condition to the next, the left-hand side of the equation is constant and has a fixed value. This implies the right-hand side of the equation is also fixed, so that any changes in one variable must be offset by equivalent changes in the other variables to maintain the constant value. The multiplier "4" in the numerator is a constant, as is π in the denominator. That means that the ratio of i to the product $d^2\alpha^2$ is also constant. Note that the brightness equation constrains the selection of the beam parameters such that all three parameters cannot be independently chosen. For example, this means that if the current i is increased by a factor of 9 but the convergence angle is unchanged, the beam diameter will increase by a factor of 3 to maintain the equality. Alternatively, if the convergence angle is increased by a factor of 2 (say, by decreasing the working distance by moving the sample closer to the objective lens) then the current can be increased by a factor of 4 without changing the beam size. Even more complex changes in the beam parameters can be understood and predicted in this way, so careful study of this equation and its implications will pay many dividends during your study of the SEM.

5.2.8 Focus

One of the first skills taught to new SEM operators is how to focus the image of the sample. From a practical perspective, all that is required is to observe the image produced by the SEM, and adjust the focus setting on the microscope until the image appears sharp (not blurry) and contains as much fine detail as possible. From the perspective of electron optics, it is not quite as straightforward to understand what happens during the focusing operation, especially if you remember that the SEM image is not formed using the action of a lens as would be the case in a light microscope, but rather by rastering a conical beam across the surface of the sample. Figure 5.5 shows the three basic focus conditions: overfocus, correct focus, and underfocus.

In the SEM the focus of the microscope is changed by altering the electrical current in the objective lens, which is almost always a round, electromagnetic lens. The larger the electrical current supplied to the objective lens, the more strongly it is excited and the stronger its magnetic field. This high magnetic field produces a large deflection in the electrons passing through the lens, causing the beam to be focused more strongly, so that the beam converges to crossover quickly after leaving the lens and entering the SEM chamber. In other words, a strongly excited objective lens has a shorter focal length than a weakly excited lens. On the left in Fig. 5.5, a strongly excited objective lens (short focal

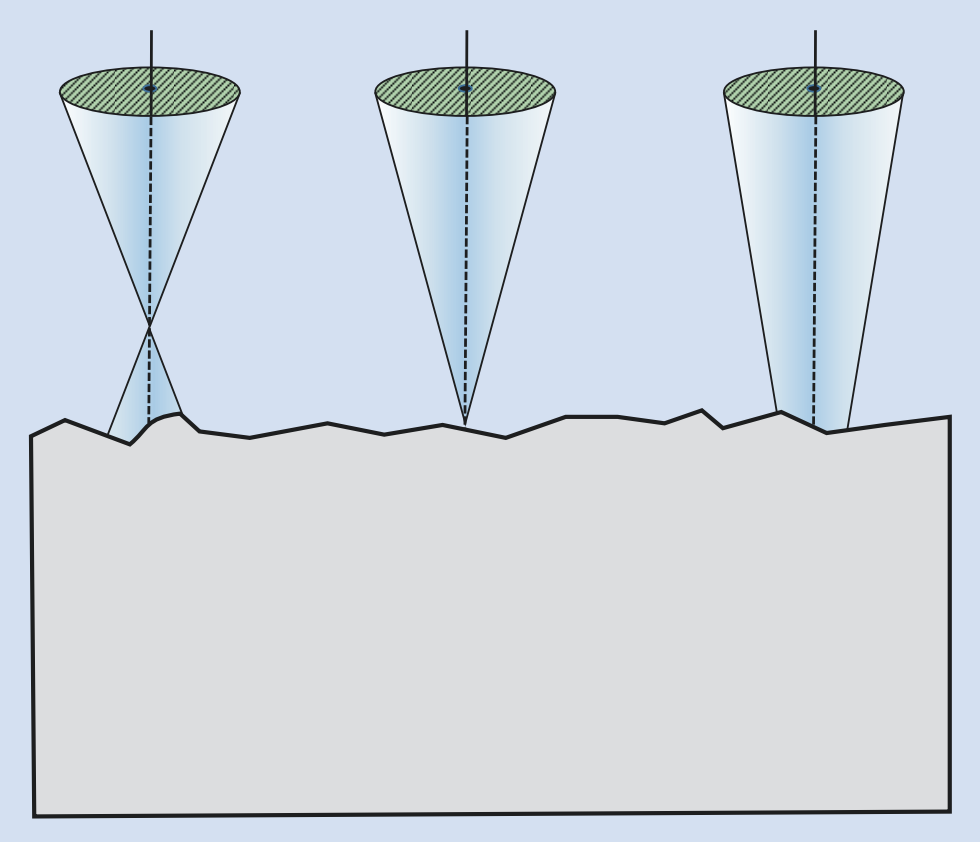

Fig. 5.5 Schematic of the conical electron beam as it strikes the surface of the sample, showing overfocus (*left*), correct focus (*center*), and underfocus (*right*). From this view it is clear that if the beam converges to crossover above the surface of the sample (*left*) or below the surface (*right*), the beam diameter is wider at the sample than the diameter of an in-focus beam (*center*)

length) causes the beam to converge to focus before the electrons reach the surface of the sample. Since the electrons then begin to diverge from this crossover point, the beam has broadened beyond its narrowest waist and is wider than optimal when it strikes the surface of the sample, thus producing an out-of-focus image. Conversely, the right-hand portion of Fig. 5.5 shows the beam behavior in an underfocused condition. Here the magnetic field is too weak, and the beam is not fully brought to crossover before it strikes the surface of the sample, and again the beam diameter is broader than optimal, resulting in an out-of-focus image.

Using these schematics as a guide, it is easier to understand what is happening electron optically when the SEM user focuses the image. Changes in the focus control result in changes in the electrical current in the objective lens, which results in raising or lowering the crossover of the electron beam relative to the surface of the sample. The distance between the objective lens exit aperture and this beam crossover point is displayed on the microscope as the working distance, *W*. On most microscopes you can see the working distance change numerically on the screen as you make gross changes in the focus setting, reflecting this vertical motion of the beam crossover in the SEM chamber. It is important to note that the term *working distance* is also used by some microscopists when referring to the distance between the objective lens pole piece and the surface of the sample. The value of *W* displayed on the microscope will accurately reflect this lens-to-sample distance if the sample is in focus.

Astigmatism

The pointy cones drawn in Fig. 5.5 are a useful fiction for representing the large-scale behavior of a focused electron beam, but if we consider the beam shape carefully near the beam crossover point this conical model of the beam breaks down. Figure 5.6 is a more realistic picture of the beam shape as it converges to its narrowest point and then begins to diverge again below that plane. For a variety of reasons, mostly the effects of lens aberrations and other imperfections, even at its narrowest point the beam retains a finite beam diameter. In other words, it can never be focused to a perfect geometrical point. The left side of Fig. 5.6 shows the beam narrowing gently but never reaching a sharp point, reflecting this reality. Ideally, cross sections through the beam at different heights will all be circles, as shown in the right of Fig. 5.6. If the beam is underfocused or overfocused, as shown in Fig. 5.5, the consequence is a blurry image caused by the larger-diameter beam (larger blue circles in Fig. 5.6 above and below the narrowest point).

In real SEMs the magnetic fields created in the electron optics are never perfectly symmetric. Although the manufacturers strive for ideal circular symmetry in round lenses, invariably there are defects in the lens yoke, the electrical windings, the machining of the pole pieces, or other problems that lead to asymmetries in the lens field and ultimately to distortions in the electron beam. Dirt or contamination buildup on the apertures in the microscope can also be an important source of distorted beam shapes. Since the dirt on the aperture is electrically non-conductive, it can

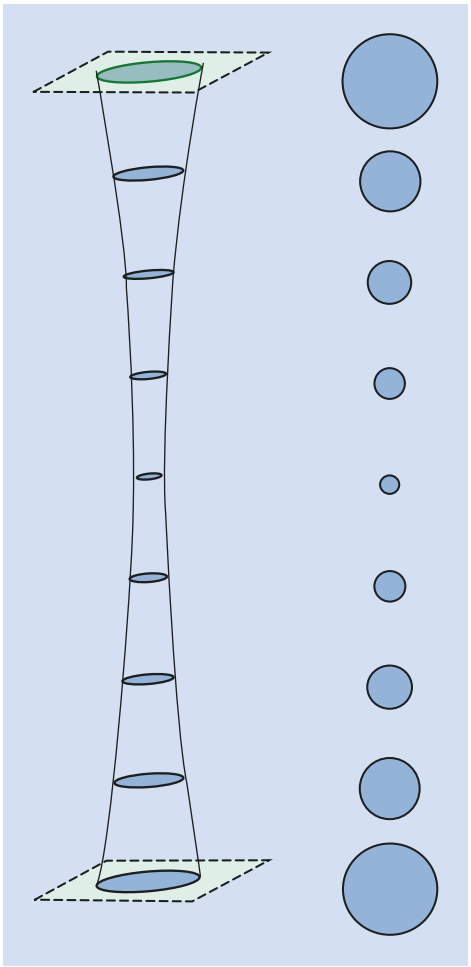

Fig. 5.6 Perspective view of the electron beam as it converges to focus and subsequently diverges (*left*), and a series of cross-sectional areas from the same beam as it travels along the optic axis (*right*). Note that although this beam does not exhibit any astigmatism it still does not focus to a point at its narrowest waist

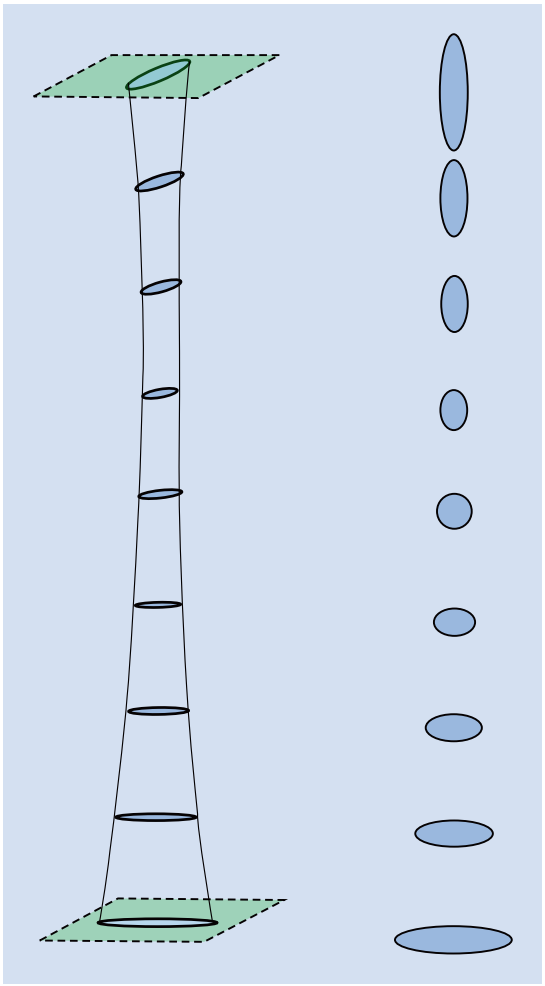

Fig. 5.7 Perspective view of an astigmatic electron beam as it converges to focus and subsequently diverges (*left*), and a series of cross-sectional areas from the same beam as it travels along the optic axis (*right*). Because this beam exhibits significant astigmatism, the cross sections are not circular and their major axis changes direction after passing through focus

accumulate an electric charge when the beam electrons strike it, and the resulting electrostatic fields can warp and bend the beam into odd and complex shapes that no longer have a circular cross section.

By far the most important of these distortions is called *two-fold astigmatism*, which in practice is often referred to just as *astigmatism*. In this specific distortion the magnetic field that focuses the electrons is stronger in one direction than in the orthogonal direction, resulting in a beam with an elliptical cross section instead of a circular one. In beams exhibiting astigmatism the electrons come to closest focus in the x-direction at a different height than the y-direction, consistent with the formation of elliptical cross sections. These effects are shown schematically in Fig. 5.7. Similar to Fig. 5.6, the focused beam is shown in perspective on the left side of the diagram, while a series of cross sections of the beam are shown on the right of the figure. In the case shown here, as the beam moves down the optical axis of the SEM, the cross section changes from an elongated ellipse with long axis in the y-direction, to a circle (albeit with a larger diameter than the equivalent circle in Fig. 5.6), and then to another elongated ellipse, but this time with its long axis oriented in the x-direction. This progression from a near-line-focus to a broader circular focus and then to a near-line-focus in an orthogonal direction is the hallmark of a beam exhibiting astigmatism.

This behavior is also easily visible in the images produced by rastering the beam on a sample. When the beam cross section is highly elongated at the surface of the sample, the image resolution is degraded badly in one direction, producing a blurring effect with pronounced linear asymmetry. It appears as if the image detail is sheared or stretched in one direction but not the other. If the focus knob is adjusted when the beam is astigmatic, a point can be reached when this image shearing or linear asymmetry is eliminated or at least greatly reduced. This is the best focus obtainable without

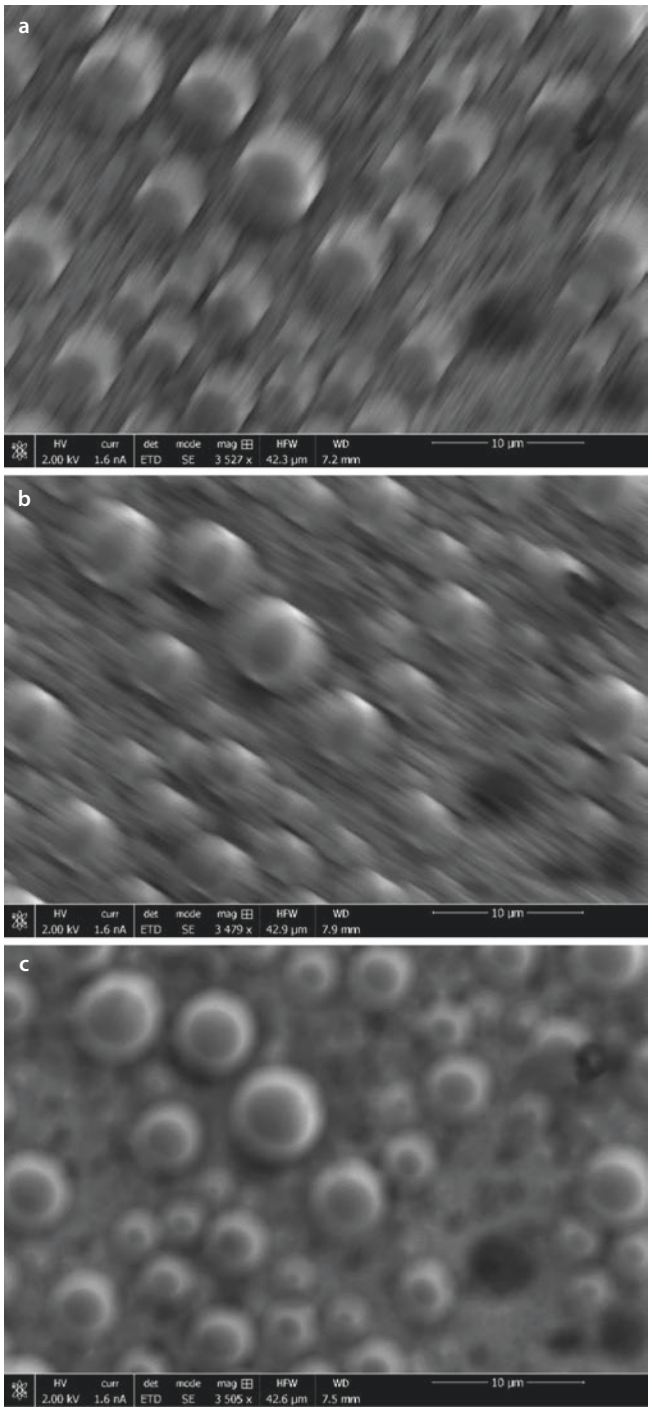

Fig. 5.8 Three SEM micrographs showing strong astigmatism in the X direction, when the sample is **a** overfocused, **b** underfocused, and **c** near focus. Note that the shearing or "tearing" appearance of fine detail in **a** appears to be in a direction perpendicular to the effect in **b**

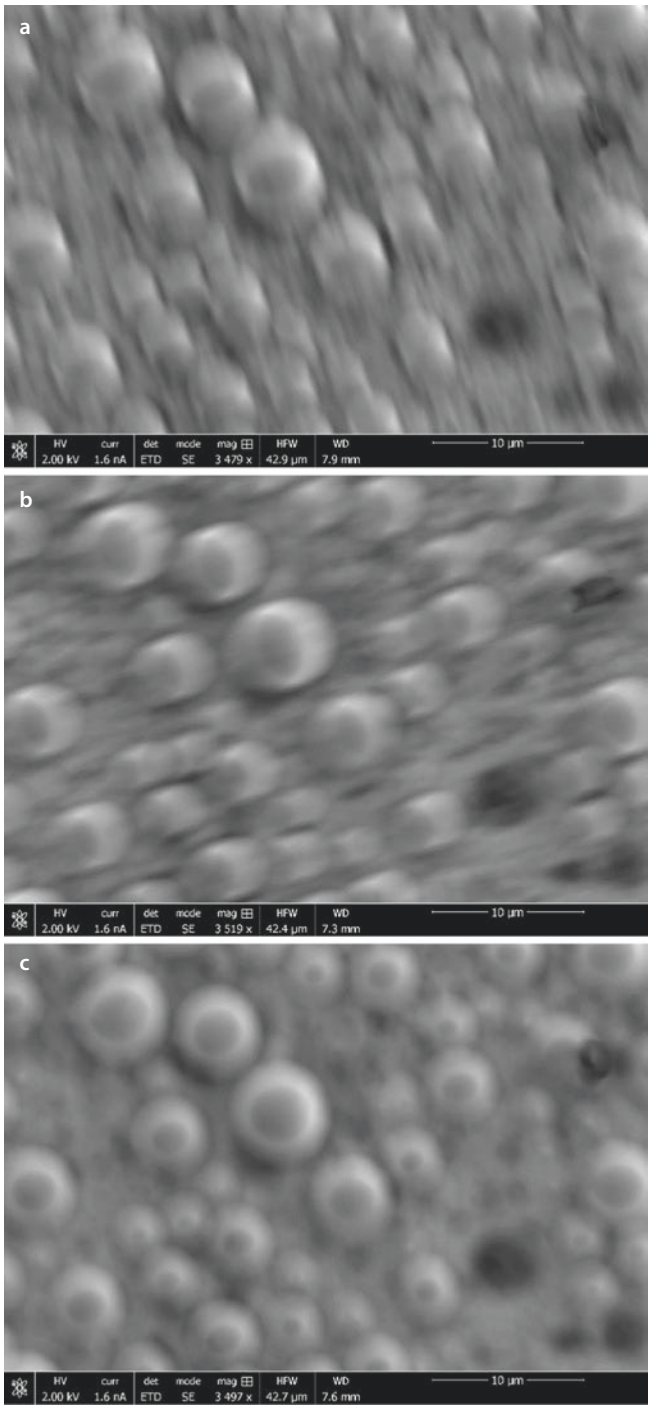

Fig. 5.9 Three additional SEM micrographs from the same field of view shown in Fig. 5.8 above. Here the beam shows strong astigmatism in the Y-direction, when the sample is **a** overfocused, **b** underfocused, and **c** near focus

correcting the astigmatism, although it generally produces an image that is far inferior to the in-focus images obtainable with a properly stigmated beam. If the focus is further adjusted, past this point of symmetry, the image will again exhibit large amounts of shearing and stretching of the fine details, but in a different direction. This sequence of effects can be seen in Fig. 5.8. In Fig. 5.8a the sample is shown when the objective lens is overfocused, with the beam crossover occurring above the sample surface, corresponding to the left diagram in Fig. 5.7. In panel Fig. 5.8b, the same sample with the same astigmatic beam is shown in underfocus, the right side diagram in Fig. 5.6. Figure 5.8c shows the best achievable focus; here, the shearing and stretching is minimized (or at least balanced), suggesting the cross section

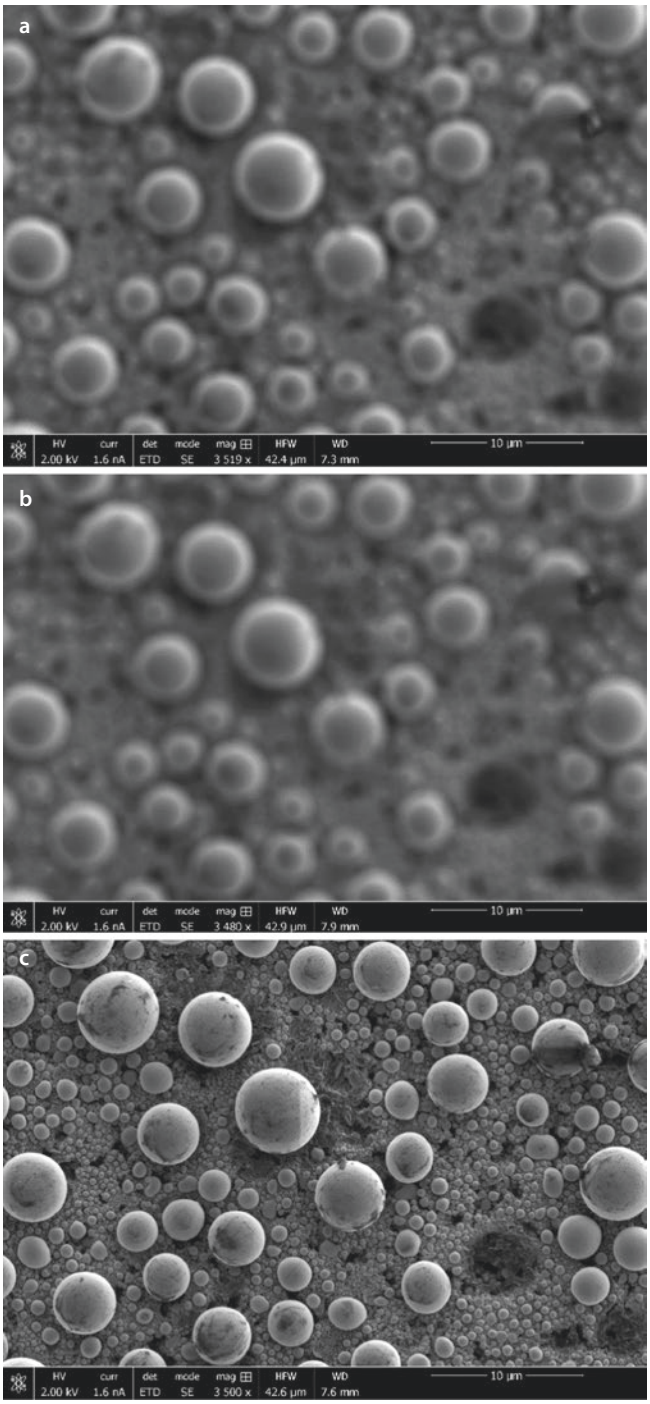

Fig. 5.10 Three additional SEM micrographs from the same field of view seen in Figs. 5.8 and 5.9 above. Here the sample is imaged with a fully corrected beam, so neither the overfocused image **a** nor the underfocused image **b** shows significant anisotropic fine detail. Further, the in-focus image in panel **c** is much sharper then the best-focus images obtained in panel **c** of Figs. 5.8 and 5.9

of the electron beam is approximately circular. Figure 5.9 shows the sample field of view seen in Fig. 5.8, but imaged using a beam with pronounced astigmatism in the Y direction. In general the SEM beam will be astigmatic in both X and Y, and the operator must correct this beam distortion along both axes using the X and Y stigmators. When this is performed correctly, a series of image like those in Fig. 5.10 can be obtained. In Fig. 5.10, both overfocused and underfocused images show loss of fine detail, but no directional distortion is present. The other significant improvement in Fig. 5.10c over Figs. 5.8c and 5.9c is that the best-focus image is much sharper when the image is properly stigmated. While this last benefit is the real reason to master the art of image stigmation, the characteristic appearance of images like those in Figs. 5.8a, b and 5.9a, b are very handy when adjusting the stigmation controls on the microscope.

Learning how to properly adjust the stigmation coils on an SEM can be one of the most challenging and frustrating skills to develop when first learning to use the instrument. However, as can be seen in the previous figures, being able to quickly and accurately minimize astigmatism in your electron micrographs is an essential milestone along the journey to becoming an expert scanning electron microscopy and X-ray microanalyst.

5.3 SEM Imaging Modes

SEMs are very flexible instruments, and the SEM operator has control over a large number of electron beam, detector, and stage parameters. Consequently, the number of different imaging conditions that may be employed to analyze any given sample is nearly infinite, and it is the job of the analyst to choose these conditions wisely to obtain useful information to meet the needs of the analysis. Fortunately, in many situations these choices can be narrowed to using one of the four basic modes of SEM operation: (1) High Depth-of-Field Mode, (2) Resolution Mode, (3) High-Current Mode, and (4) Low-Voltage Mode.

Below you will find practical information on how to control the fundamental electron optical parameters described earlier in the text and specific guidance for operating the SEM in the four basic modes just mentioned. Experienced SEM operators will have mastered these four modes and will be comfortable moving between them as needed. Choosing any one of these modes is a compromise, since each of them sacrifices microscope performance in some areas to achieve other imaging goals. Appreciating the strengths and weaknesses of each mode is essential to understanding when each mode is warranted. Of course some analyses will demand imaging conditions that do not fall neatly into one of these four basic modes, and the expert SEM operator will use the full flexibility of the instrument when required.

5.3.1 High Depth-of-Field Mode

Anyone familiar with compound light microscopes (LMs) understands that they have a very limited Depth-of-Field (DoF), meaning there is a limited range of vertical heights on the sample surface that will all appear to be in focus simultaneously. Parts of the sample that fall outside this range appear blurry. One of the advantages of the SEM over the light microscope is that it is capable of a much deeper depth-of-field than the LM.

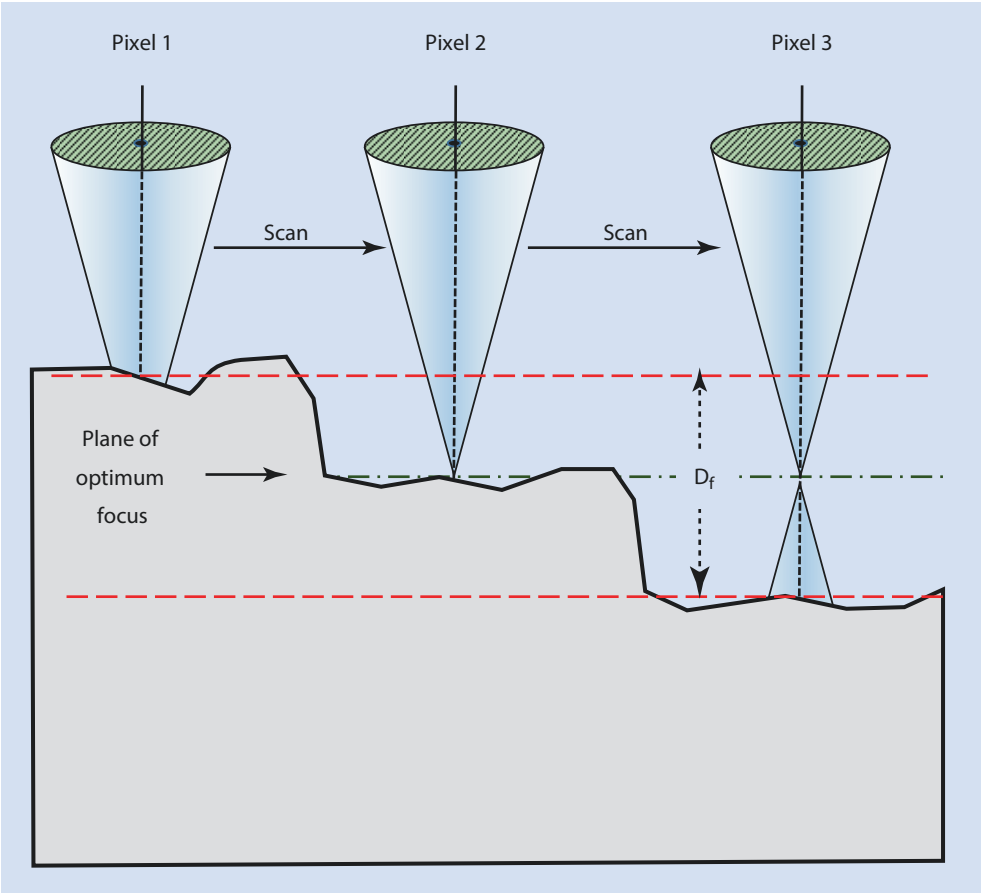

Fig. 5.11 Schematic showing why an SEM has finite depth-of-field D_f and how it is defined

The shallow depth-of-field in the LM arises from the properties of its glass lenses, but SEMs don't use lenses to form direct images; instead they rely on lenses to focus the beam and then scan this beam from pixel to pixel to image the sample.[1] Nonetheless, they suffer from limited DoF because of the effect shown schematically in Fig. 5.11. Here the electron beam is shown striking the sample in three different locations, producing three different pixels in the image. For all three pixels the vertical position of the electron beam crossover is the same; this height is called the plane of optimum focus and is represented in Fig. 5.11 as a horizontal green dot-dashed line. For the case of pixel 2, this plane coincides with the surface of the sample. For pixel 1, the electron beam has not yet reached crossover when it strikes the surface of the sample, at a height denoted by the upper red dotted line. This is equivalent to underfocusing the beam, with the same effect: the diameter of the probe at the sample surface is larger than optimal. If this increase in probe size is large enough, it will degrade the sharpness of the image. The height at which this blurring becomes measureable, denoted by the upper red dotted line, is the upper limit of the DoF for this beam. Similarly, for pixel 3 the sample surface is lower (i.e., further from the objective lens) than the middle case. This is analogous to overfocus because the beam comes to crossover and begins to diverge again before it lands on the sample. As before, this can degrade the sharpness of the image, and the height at which this degradation is noticeable is the lower limit of the height range that defines the DoF. The distance between these two dotted red lines is labeled D_f in Fig. 5.11, denoting the depth-of-field.

Because the definition of DoF requires the resulting blur to be noticeable (or at least measureable), it depends on many factors and can be somewhat subjective. For example, since in most cases sub-pixel blurring is not a concern to the SEM analyst, the effective DoF will often improve as the magnification decreases and the pixel size increases. However, as the magnification decreases, much more of the sample is visible in the field of view, increasing the chances that pronounced topography will lead to blurring. In these cases the DoF is

1 Glass lenses and transmission electron microscope lenses also have a related property known as *depth-of-focus*, a term that is often confused with depth-of-field. Depth-of-field refers to the range of heights in simultaneous focus *on the sample* (i.e., the observed field). In contrast, depth-of-focus refers to the range of positions near the imaging plane of the lens where the image is in focus. This determines, for example, how far away from the ideal imaging plane of the lens you can place a piece of film, or a CCD detector, and still capture an in-focus image. Because SEMs capture images via scanning action, the term depth-of-focus is not relevant.

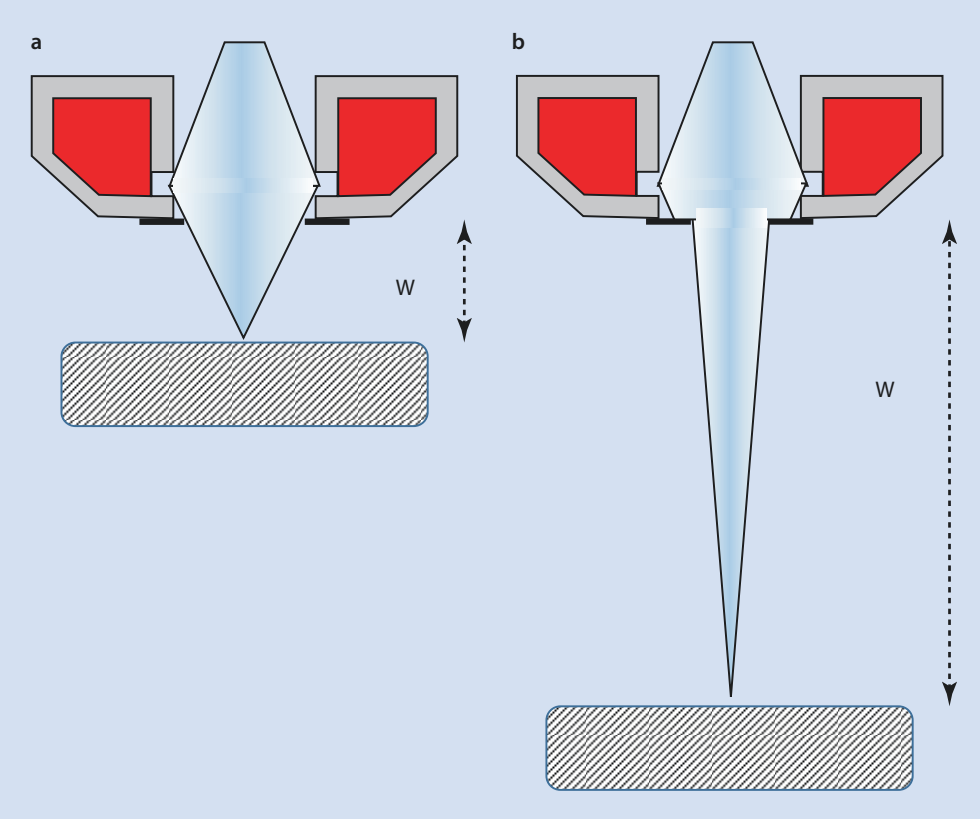

Fig. 5.12 **a** Diagram of the electron beam emerging from the final aperture in the objective lens and striking the sample under typical imaging conditions; a relatively large aperture diameter and short working distance create a large convergence angle and therefore a shallow depth-of-field. **b** *High Depth-of-Field Mode.* Here a small aperture diameter and long working distance *W* combine to create a small convergence angle and therefore a large depth-of-field

still increased at low magnification, but parts of the sample are still blurred in the image because of the large range of height visible in the expanded field of view. Nonetheless, operating the SEM in High Depth-of-Field Mode at medium to low magnifications is perhaps the most often used imaging condition for routine SEM work.

The basic idea behind High Depth-of-Field Mode is to create a set of imaging conditions where the convergence angle of the beam is small, producing a narrow pencil-like electron beam that does not change diameter rapidly with height above the sample. Figure 5.12 shows what this looks like schematically. Figure 5.12a represents typical imaging conditions, with short working distance W and normal aperture diameter. Figure 5.12b shows the imaging conditions used in High Depth-of-Field Mode, where the working distance has been increased significantly and a smaller diameter aperture is inserted. These two changes decrease the convergence angle of the electron beam and therefore increase the DoF. The effects of the aperture and working distance are independent of each other, meaning either one can improve the depth-of-field by itself.

For best results in Depth-of-Field Mode, determine the lowest stage position available (largest working distance), and drive the sample to that location. Changing the working distance is straightforward on most SEMs. Those microscopes with a manual stage will often have a physical knob on the chamber door for changing the height of the sample. Motorized stages are sometimes controlled by a hand panel, joystick, or stand-alone stage controller, especially on older microscopes. Recent models typically use a graphical user interface, requiring the operator to enter a destination height (or "Z position") in millimeters and then executing the move. Some also allow the stage height to be changed continuously using the mouse.

Depth-of-Field Mode is also optimized by selecting a relatively small final beam aperture. The mechanisms used to change the diameter of the final aperture, and to center it on the optical axis of the microscope, vary widely from one SEM model to the next. In fact, some SEMs are designed to use a fixed or semi-fixed final aperture and do not provide an easy method of altering the aperture size. Many microscopes have manual aperture controls mounted on the outside of the SEM column (Fig. 5.13). Other microscopes use a graphical user interface (GUI) to allow the operator to select one of several available apertures for insertion. Following this selection, motors driven by an X/Y- motion controller physically move the selected aperture into place and recall from memory the X- and Y- positions needed to center it. In either case the apertures themselves are arrayed linearly as a series of circular holes in a long, thin aperture strip.

A few microscopes permit you to configure Depth-of-Field Mode directly by selecting this option in the instrument control software. Figure 5.14 shows an example screenshot from one manufacturer's user interface where the operator can select a dedicated "DEPTH" setting, automatically optimizing the instrument for a small convergence angle.

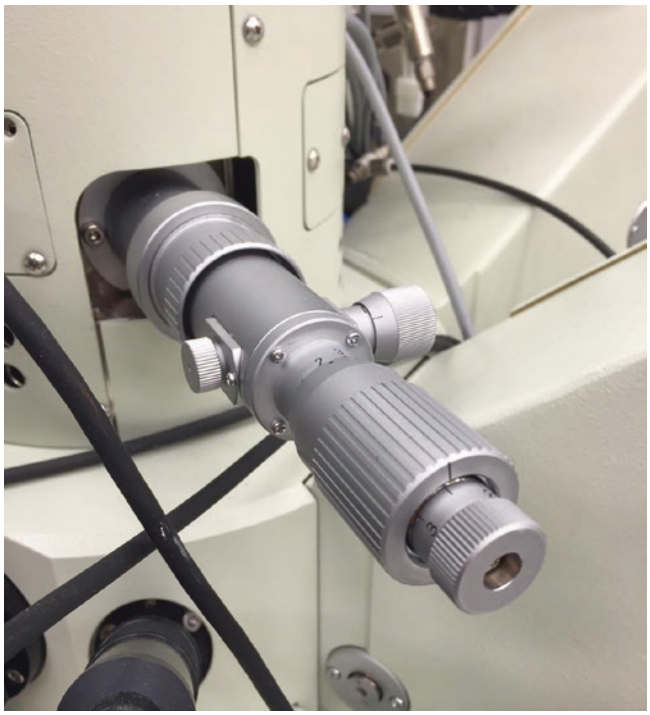

Fig. 5.13 Manual aperture control mounted on the outside of an electron optical column. This mechanism allows the operator to select one of several different discrete apertures and adjust the X- and Y-positions of the aperture to center it on the optical axis of the microscope

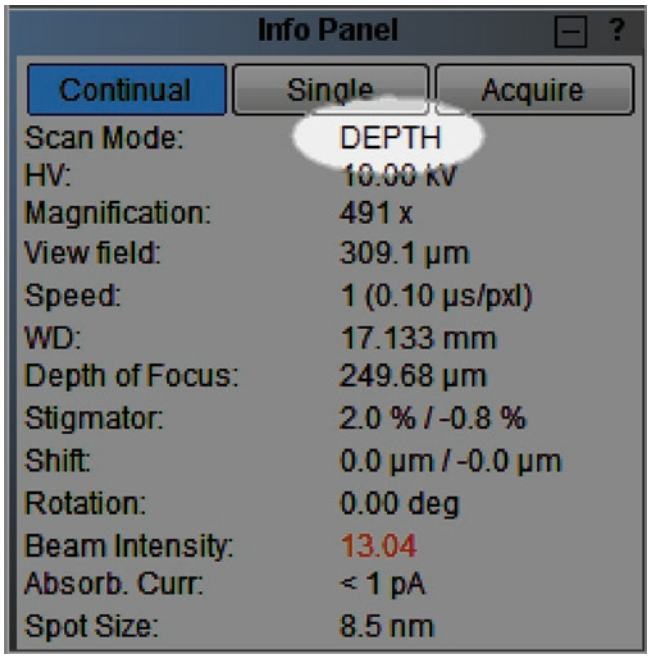

Fig. 5.14 Graphical user interface from one manufacturer's instrument control software that allows the user to select Depth-of-Field Mode directly. On this microscope, once the Scan Mode is set to "DEPTH," the electron column is configured automatically to create a small convergence angle and a large depth-of-field

5.3.2 High-Current Mode

Like the High Depth-of-Field Mode described above, the High-Current Mode of operating the SEM is used frequently. In many common imaging situations it delivers excellent feature visibility, useful and informative materials contrast, and adequate resolution and depth-of-field . It is particularly useful when the native contrast of the sample is low, such as when neighboring materials phases exhibit approximately equal average atomic number. It is also invaluable when performing X-ray microanalysis since the higher beam current translates directly into higher X-ray count rates. This can help by shortening the acquisition time needed to acquire individual X-ray spectra with an adequate number of counts for quantitative analysis, but it is even more important when acquiring X-ray maps or spectrum image datasets with full spectra at every spatial pixel. In all the cases mentioned above, feature visibility and count rate (both enabled by high current) are more important than spatial resolution or depth-of-field .

The basic idea behind High-Current Mode is to increase the current in the probe to boost both the signal reaching the detectors and the signal-to-noise ratio. Regardless of the electron detector in use (e.g., Everhart–Thornley detector, dedicated backscatter detector, through-the-lens detector, etc.), the signal reaching the detector scales with the signal generated at the sample, and this in turn scale directly with the current in the electron probe.

Unfortunately, the controls used to vary the electron beam current vary widely from one SEM model to the next, and different SEM manufacturers use discordant or conflicting terminology to describe these controls. As dictated by the brightness equation, the probe diameter must increase with an increase in probe current, so some manufacturers call the control "Spot Size." On some microscopes Spot Size 1 is a small spot (corresponding to a low beam current) and Spot Size 10 is a large spot (high current); a different vendor, however, may have adopted the convention where Spot Size 1 is a large spot and Spot Size 10 is a small spot. Other companies use the term *Spot Size,* but specify it in nanometers in an attempt to represent the nominal diameter of the probe. An approach growing in popularity with more modern instruments is to allow the operator to set the nominal probe current itself instead of Spot Size. As discussed above, this can be done either in discrete steps or continuously. In either case, the current steps can be labeled with arbitrary numbers (e.g., 7), they can reflect the nominal probe current (e.g., 100 pA), or sometimes they are specified as a percentage of the maximum current (e.g., 30 %). This dizzying variety of methods for labeling the desired probe current on SEMs can be confusing when switching from one instrument to another.

Figure 5.15 shows two different varieties of physical knob configuration that might be encountered on the control panel of SEMs and electron probe microanalyzers (EPMAs). These analog controls are very intuitive to use because turning the knob changes the beam current in an immediate and continuous manner, allowing fine control of this parameter. Large

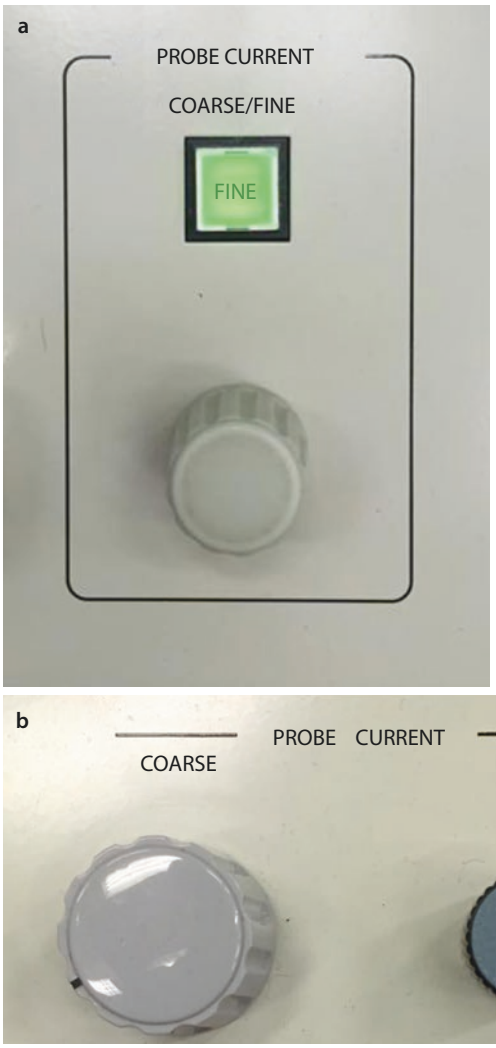

Fig. 5.15 Examples of physical knobs on SEMs and electron probe microanalyzers (EPMAs) used by the operator to adjust the beam current. In both cases the operator has access to a coarse and a fine adjustment, either using one knob and a coarse/fine selector button **a**, or dedicated knobs for coarse and fine control **b**

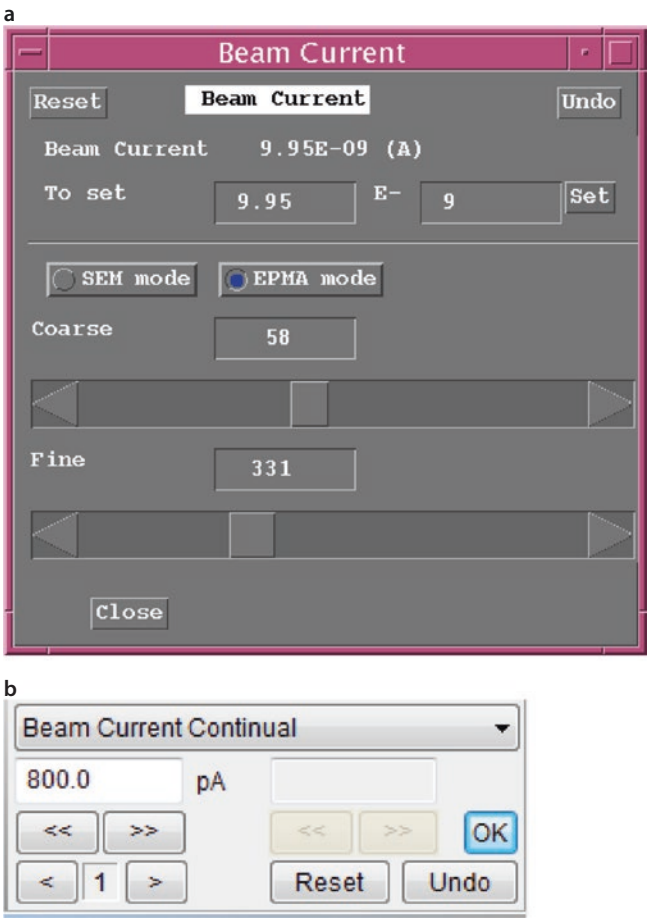

Fig. 5.16 Examples of graphical user interface controls present in different manufacturers that allow the operator to control the beam current continuously. In **a**, the operator has a choice of setting the nominal current in pA digitally, or by using coarse and fine slider controls expressed in arbitrary units. In **b**, the operator also has a nominal beam current control expressed in pA as well as buttons to increase to decrease the value

changes in beam current can be made quickly by using the coarse setting of the knob shown in Fig. 5.15a, or the coarse knob shown in Fig. 5.15b. In both cases fine control is also possible for smaller adjustments. Figure 5.16 shows two examples of computer-based beam current controls of the type found in graphical user interfaces. In both cases the operator can change the beam current using the mouse and keyboard. In Fig. 5.16a this can be accomplished either by entering an exact digital value for the beam current and clicking the "Set" button, by dragging one of the two the slider controls to the left or right, or by clicking the arrow buttons to increase to decrease the current setting. Note that on this microscope, the slider positions are expressed digitally using arbitrary units (58 units for the coarse slider and 331 units for the fine slider). While these numbers are not true current values, these arbitrary settings can be useful for returning the microscope to a specific current. Figure 5.16b shows a similar GUI window from the user interface written by a different manufacturer. In this case, the operator also has access to a numerical beam current setting, nominally calibrated in true current measured in pA, as well as buttons that when clicked will increase or decrease the beam current incrementally. Finally, Fig. 5.17 shows screenshots from a graphical user interface based on Spot Size instead of beam current. The operator is asked to select a specific Spot Size using a quick access pull-down menu (Fig. 5.17a) or a more flexible combination of a pull-down menu and up/down buttons (Fig. 5.17b). While these figures provide a sampling of the large variety of terms and interface layouts that the operator might encounter in the field, there are many more variations in practice than can be shown here.

Regardless of how any given SEM allows the operator to change the probe current, the most important tasks for the operator are to know how to increase and decrease current, and how to measure the current accurately once set. Even on those instruments that let the operator select a numerical probe current (e.g., 1 nA) via the user interface, it is unwise

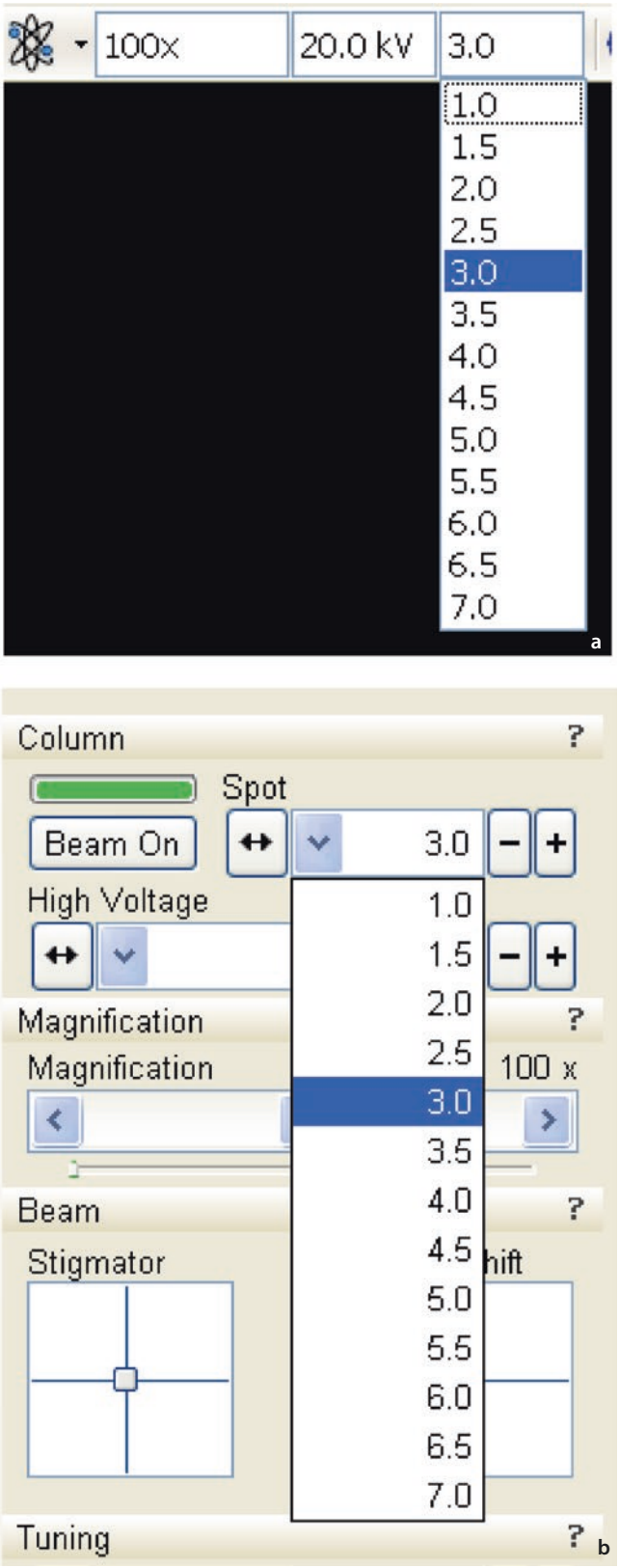

Fig. 5.17 Examples of graphical user interface controls that allow the operator to control the beam current in discrete steps expressed as changes in Spot Size. In **a**, the can choose any of several Spot Size values from a pull-down menu. In **b**, from the same microscope, the operator can access Spot Size via a pull-down menu or buttons that increase or decrease the value

to assume this setting will reliably produce the displayed value. Well-equipped SEMs have a built-in picoammeter that can be automatically inserted into the beam path to measure probe current. Getting a reading in these cases is as simple as triggering the insertion of the meter's cup and reading the value off the screen. Alternatively, a stage-mounted Faraday cup (either purchased commercially or homemade) attached through an electrical feedthrough to a benchtop picoammeter can be used instead.

Since the basic idea of High-Current Mode is to deliver sufficient probe current to the sample to generate superior signal-to-noise ratio, optimum results are obtained at medium to low magnifications, and often a larger final aperture is useful. Frame the field-of-view desired, focus the beam, and increase probe current until high-quality images can be obtained within a relatively short frame time, say, a few seconds to a minute. Check that any low-contrast features needed for analysis are sufficiently visible, and increase probe current further if they are not. For many situations, this high-current imaging approach will yield excellent images quickly and with little wasted time. If you are performing X-ray microanalysis, the approach to High-Current Mode is very similar to that for imaging, but the choice of current is dictated not by image quality but by X-ray count rate or, more suitably, the dead time percentage of the X-ray spectrometer's pulse processor.

5.3.3 Resolution Mode

Resolution Mode is probably the most demanding of the four basic SEM operational modes, chiefly because the microscope is driven at or near its limits of performance. It challenges the operator mentally, since choosing optimum imaging parameters requires deeper knowledge of electron optics and the physics of electron beams, although suitable images can be obtained with a basic understanding of the principles. It also demands more skill in operating the microscope, since small misalignments (e.g., residual stigmatism, imperfectly centered aperture) are more apparent. In fact, good alignment of the entire column is necessary to get the best resolution from the scope, while small misalignments are often tolerated in High-Current or High Depth-of-Field Mode. Resolution Mode also expects more from the microscope's environment. Mechanical vibrations, electronic noise, and AC magnetic fields near the microscope are some of the many sources of image degradation that, while generally unnoticeable, become obvious when operating in Resolution Mode. Poor sample preparation, such as overly thick evaporated metal coatings or insufficient metallographic polishing, for example, is also more evident at high magnifications. Most of these challenges are greatly reduced at lower magnifications, but the larger pixel sizes that result from low magnification obviate the need for Resolution Mode. In short, the same imaging conditions that enable Resolution Mode also highlight any shortcomings in the operator's technique, the laboratory environment, and the sample preparation.

Although every one of the basic SEM operational modes requires some compromise, in Resolution Mode the pursuit of high spatial resolution often involves compromise across the board. Small probe diameters require very low beam currents, thereby reducing the signal generated and lengthening the frame times needed. Depth-of-field is also reduced, although this is often not noticeable at high magnification, and detector choice is usually limited to the one or two channels optimized for this purpose (e.g., through-the-lens detectors).

The basic idea in Resolution Mode is to (1) minimize the probe diameter by raising the beam energy and reducing the beam current, (2) emphasize the collection of the resolution-preserving SE_1 secondary electrons generated at the beam footprint, and (3) minimize the myriad sources of image degradation by using the shortest working distance possible. Raising the beam energy helps produce smaller probe sizes because it increases the brightness of the gun. For thin samples, such as small particles sitting on an ultrathin film substrate, this produces the highest resolution. Likewise for very high-Z samples, even high landing energies have short electron ranges and therefore small excitation volumes. However, for thick samples with low atomic number, better resolution may be obtained at lower landing energies if the size of the excitation volume is the limiting factor. For any given beam energy, smaller currents always yield smaller probe sizes, as demanded by the brightness equation, so operating at tens of picoamps is not uncommon in this mode. Choice of signal carrier and detector can be crucial for obtaining high spatial resolution. Since backscattered electrons emerge from a disc comparable in size to the electron range, it is very hard to realize high resolution by using backscattered electrons (BSE) directly or BSE-generated secondaries such as SE_2 secondary electrons (generated at the sample surface by emerging BSE) or SE_3 secondary electrons (generated at great distance from the sample by BSE that strike microscope components). The highest resolution is obtained from SE_1 secondary electrons, because these emerge from the very narrow electron probe footprint on the sample surface, comparable in diameter to the probe itself. Microscopes equipped with immersion objective lenses or snorkel lenses and through-the-lens detectors (TTLs) are best at efficient collection of SE_1 electrons. Finally, bringing the sample very close to the objective lens, even less than 1 mm if practical, can improve resolution significantly. SE_1 collection is maximized by this proximity, and a short working distance (WD) can minimize the length over which beam perturbations such as AC fields can act.

The practical steps needed to configure the SEM for operation in Resolution Mode follow from the basic requirements outlined above. Get the sample as close to the objective lens as possible by carefully shortening the working distance. Computer-controlled SEMs will frequently have a software interlock designed to reduce the chances that the sample will physically impact the pole piece. Learn how this feature functions and use it effectively but carefully; high resolution is useful, but a scratched or dented pole piece can be a very expensive mistake! Also, beware that many microscopes possess more than one objective lens mode. Invariably the lens mode needed for best resolution will be the one that creates the highest magnetic field at the sample. Coupled with the proximity of a short working distance, these high magnetic field modes may lift your sample off the stage unless it consists of a non-magnetic material. Select the TTL detector if available, or other detector that preferentially utilizes SE_1 secondary electrons for imaging. Increase the accelerating voltage on the SEM to its highest setting, usually 30 kV or higher, and reduce the beam current to as low a value as practical while still maintaining visibility of the sample as noise increases. Moving to a slower frame time, longer dwell time, or enabling frame averaging will help mitigate the effects of reduced signal at low probe currents. Finally, select the optimal objective lens aperture diameter for best resolution. This can be tricky because of competing effects. Small apertures can limit the resolution due to diffraction effects, so the larger the aperture the less likely that these effects will be a problem. However, large apertures quickly amplify the effects of objective lens aberrations, especially spherical aberration, so the smallest aperture size available is ideal for reduction of aberrations. Clearly these requirements conflict with one another, and every objective lens has an intermediate aperture diameter that delivers the best resolution for any given beam energy and working distance. Some SEMs inform the operator of this optimal aperture size, while others are less helpful and leave it up to the operator to determine the best choice. In these cases, contact the SEM manufacturer's application engineer for advice or test a variety of aperture diameters on high quality imaging test specimens to understand how to manage this tradeoff.

5.3.4 Low-Voltage Mode

Of the four basic SEM modes, Low-Voltage Mode is probably the most esoteric and challenging, regarding both instrumentation and specimen issues. Reducing the landing energy of the beam is useful in many situations, and varying the beam energy should be considered when operating in High-Current Mode or Depth-of-Field Mode as needed. However, operating with landing energies below 5 keV, and especially below 1 keV, is qualitatively different than using higher energies. The performance of the SEM's entire electron optical chain, from the electron gun to the objective lens, is much worse at 1 keV than at high beam energy. While modern thermionic SEMs are often quite good performers in Low-Voltage Mode, not many years ago a field emission electron source (FEG) was considered a de facto requirement for low voltage work, and most older thermionic SEMs produce such poor images at 1 keV that they are almost useless.

For all electron sources the gun's brightness will be much lower at 1 keV than at 30 keV, which limits the current density in the probe because of the brightness equation. This in turn means the operator must work at much larger probe sizes to obtain sufficient current for imaging. Here field emission sources have a big advantage over tungsten or LaB_6 thermionic filaments because they are much brighter intrinsically, and so remain bright enough at low voltage for decent imaging. Another important concern that arises at these low beam

energies is the chromatic aberration of the objective lens. This aberration causes beam electrons at different energies to be focused in different planes, reducing the current density. Although this aberration is a flaw in the lens itself and not the electrons in the beam, lower beam energies make the problem more apparent, in part because they have a larger fractional energy spread. In fact, the effects of this aberration would not be noticeable at all in a monochromatic electron beam, where all the electrons have exactly the same energy. Similarly, electron sources with naturally narrow energy spreads, such as cold field emission sources, suffer from these problems much less than sources with large energy spreads like thermionic guns. Whatever their cause, these reductions in image quality, both lower resolution and lower current density, explain why Low-Voltage Mode is commonly employed at low magnifications. Operators with expensive, high-performing field emission microscopes designed for low voltage operation will be able to work at low voltage and high magnification—even more so if the microscope is equipped with a beam monochromator, an accessory designed to artificially narrow the energy spread of the electron beam, thus reducing the effect of chromatic aberration even at very high magnifications.

Another unwanted consequence of using very low beam energies is that the resulting electron trajectories are less "stiff," meaning the electrons are more easily deflected from their intended paths by stray electric or magnetic fields near the beam. At 1 keV landing energy and below, the electrons are moving relatively slowly and are more susceptible to electrical charging in the sample, AC electric or magnetic fields in the microscope room, and electrical noise on the microscope's scan coils. These are some of the many challenges of imaging in Low-Voltage Mode.

The main advantages of Low-Voltage Mode are the much-reduced excitation volume and the resulting change in contrast for most sample materials. The range of primary beam electrons in most materials drops very rapidly as the landing energy is reduced, so the region in the sample emitting signal-carrying electrons can be very small, improving resolution in cases where it is limited by this range. The resulting surface sensitivity of the signal also tends to flatten the image contrast and it de-emphasizes materials contrast in favor of topography. Because the view of the sample in Low-Voltage Mode is often dramatically different than the equivalent image at normal beam energy, this mode often reveals important features in the sample that might be missed using routine imaging conditions.

It is possible to perform X-ray microanalysis at low voltage, but it presents special challenges and should not be attempted unless it is unavoidable. The very short electron range means the X-rays produced in the sample are generated close to the surface and very near the beam impact point. This is a good thing, because both lateral and depth resolution are improved, and absorption losses are reduced for outgoing X-rays. However, the low landing energies severely limit the number of X-ray lines that are efficiently excited, and many elements are either inaccessible, or the analyst is forced to use M- or N-shell lines with poorly measured cross sections or absorption coefficients. Complicating matters further, the reduced brightness at low voltage means probe currents are low and X-ray count rates can be anemic.

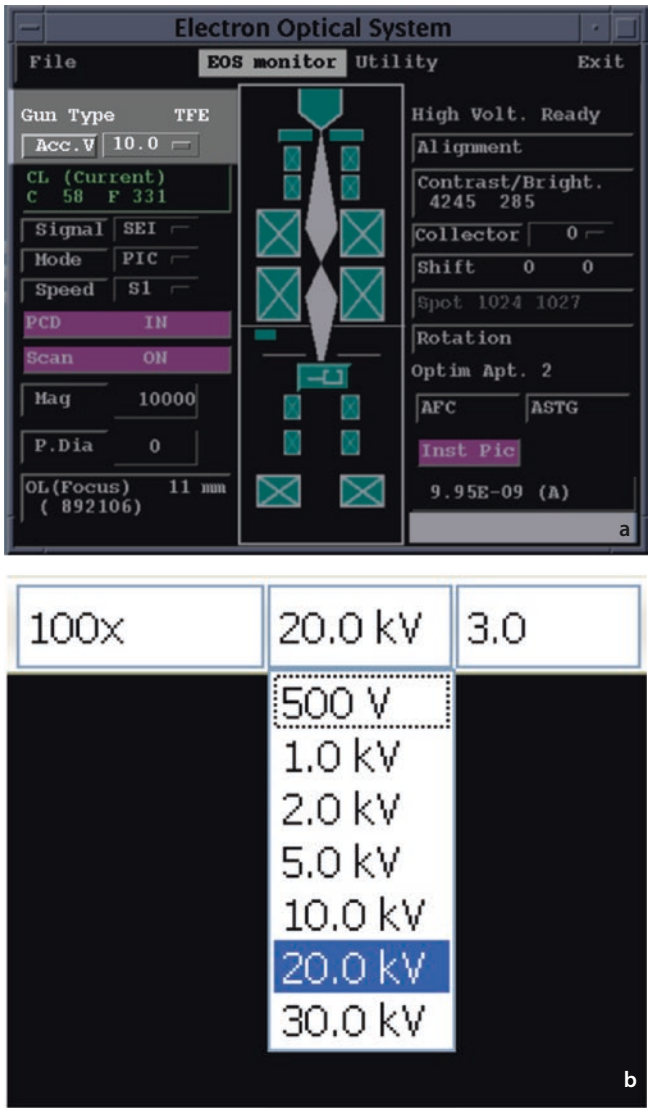

Fig. 5.18 Graphical user interface controls that allow the operator to control the beam energy. The instrument control software shown in **a** utilizes a pull-down menu on the *upper left* of the window to allow the operator to select the accelerating voltage in kilovolts (and thus the beam energy in kilo-electronvolts). The control is currently set to 10 kV. The interface in the screenshot in **b** shows a drop-down menu, allowing the SEM operator to select one of several discrete accelerating voltages between 500 V and 30 keV. In most cases, including the two shown above, the microscope allows the user to select values between the discrete settings shown in the screenshots, via a different mechanism (not shown)

The basic idea behind low voltage mode is simple: reduce the landing energy of the beam. The practical advice for configuring this mode is equally straightforward, since changing the beam energy on most microscopes is controlled by a dedicated knob or can be achieved by selecting the desired energy on a graphical user interface. Figure 5.18 shows two examples of GUI controls from different instruments. In screenshots the controls are expressed in accelerating voltage measured in kV; this is equivalent to controlling the beam energy in keV.

In some cases the SEM may allow the operator to apply a sample bias or use another form of beam deceleration, thus permitting the electron landing energy to differ from the beam energy. In these situations the manufacturer's instrument manual should be consulted for exact configuration guidance, and it is important to remember that it is the landing energy (not the energy of the beam as it leaves the objective lens) that governs both the electron range and the X-ray generation physics.

5.4 Electron Detectors

The SEM is equipped with one or more detectors that are sensitive to BSE, SE, or a combination of BSE and SE that emerge from the specimen as a result of the interaction of the primary electron beam. By measuring the response of BSE and SE as a function of beam location, various properties of the specimen, including composition, thickness, topography, crystallographic orientation, and magnetic and electrical fields, can be revealed in SEM images.

5.4.1 Important Properties of BSE and SE for Detector Design and Operation

Abundance

The total yield per incident beam electron of BSE or SE is sensitive to specimen properties such as the average atomic number (BSE), the chemical state (SE), local specimen inclination (BSE and SE), crystallographic orientation (BSE), and local magnetic field (BSE and SE). However, the total electron signal is not what is measured by most electron detectors in common use for SEM imaging. The actual response of a particular detector is further complicated by its limited angular range of acceptance as well as its sensitivity to the energy of the electrons being detected. The only detector which is exclusively sensitive to the number of BSE and/or SE (and not emitted trajectory or energy distributions) is the specimen itself when the specimen current is used as an imaging signal.

Angular Distribution

Knowledge of the trajectories of BSE and SE after leaving the specimen is important for placing a detector to intercept the useful signals. For a beam incident perpendicularly to a surface (i.e., the beam is parallel to the normal to the surface), BSE and SE are emitted with the same angular distribution which approximately follows the cosine function: the relative abundance along any direction is proportional to the cosine of the angle between the surface normal and that direction. Thus, the most abundant emission is along the direction parallel to the surface normal (i.e., back along the beam, where the angle = 0° and cos *0*° = 1.0), while relatively few BSE or SE are emitted close to the surface (e.g., along a direction 1° above the surface is 89° from the surface normal, cos 89° = 0.017, so that only 1.7 % is emitted compared to the intensity emitted back along the beam). When a surface is highly inclined to the beam, the angular distribution of the SE still follows the cosine distribution, but the BSE follow a distribution that becomes progressively more asymmetric with tilt and is peaked in the forward (down slope) direction. For local surface inclinations above approximately 45°, the most likely direction of BSE emission is at an angle above the surface that is similar to the beam incidence angle above the surface. The directionality of BSE emission becomes more strongly peaked as the inclination further increases.

Kinetic Energy Response

BSE and SE have sharply differing kinetic energies. BSE retain a significant fraction of the incident energy of the beam electrons from which they originate, with typically more than 50 % of the BSE escaping while retaining more than 0.5 E_0. The BSE coefficient, the relative abundance of energetic BSE, and the peak BSE energy all increase with the atomic number of the target. Thus, for an incident beam energy of $E_0 = 20$ keV, a large fraction of the BSE will escape with a kinetic energy of 10 keV or more. By comparison, SE are much lower in kinetic energy, being emitted with less than 50 eV (by arbitrary definition). In fact, most SE exit the specimen with less than 10 eV, and the peak of the SE kinetic energy distribution is in the range 2 eV to 5 eV. Methods of detecting electrons include (1) charge generation during inelastic scattering of an energetic electron within semiconductor devices and (2) scintillation, the emission of light when an energetic electron strikes a suitably sensitive material, which includes inorganic compounds (e.g., CaF_2 with a minor dopant of the rare earth element Eu), certain glasses incorporating rare earth elements, and organic compounds (e.g., certain plastics). Both charge generation in semiconductors and scintillation require that electrons have elevated kinetic energy, typically above several kilo-electronvolts, to initiate the detection process, and the strength of the detection effect generally increases with increasing kinetic energy. Thus, most BSE produced by a beam in the conventional energy range of 10–30 keV can be directly detected with semiconductor and scintillation detectors, while these same detectors are not sensitive to SE because of their much lower kinetic energy. To detect SE, post-specimen acceleration must be applied to boost the kinetic energy of SE into the detectable range.

5.4.2 Detector Characteristics

Angular Measures for Electron Detectors

Key Fact

Knowledge of the location of electron detectors is critical for proper interpretation of SEM images, especially of topographic features. Apparent illumination in the SEM image appears to come from the detector, while the observer's view appears to be along the incident electron beam, as discussed in detail in the Image Formation module.

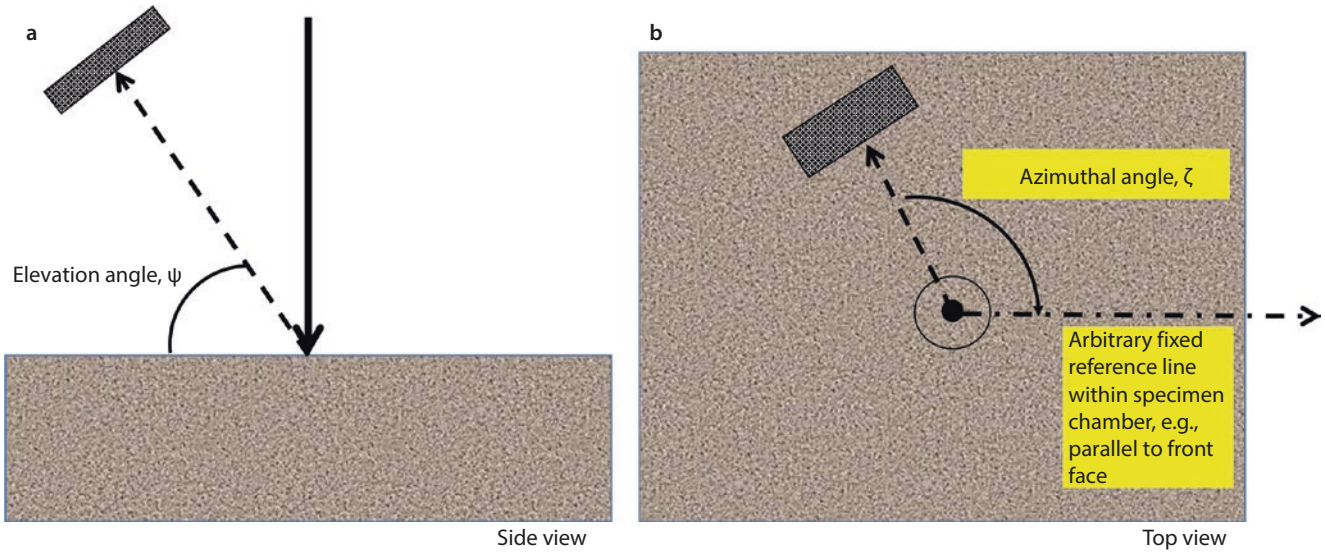

Fig. 5.19 **a** Detector take-off angle, ψ. **b** Detector azimuthal angle around beam, ζ

Elevation (Take-Off) Angle, ψ, and Azimuthal Angle, ζ

The effective position of a detector is specified by two angles. The *elevation* ("*take-off*") *angle*, designated ψ, is the angle above a horizontal plane perpendicular to the beam axis and the vector that joins the center of the detector to the beam impact position on the specimen, as shown in Fig. 5.19a. (Alternatively, the take-off angle can be measured as the complement of the angle between the beam axis and a line perpendicular to the detector face extended to the beam optic axis.) The "*azimuthal angle,*" ζ, of the detector is the rotational angle around the beam to the detector line, measured relative to some arbitrary but fixed reference, such as the front face of the specimen chamber, as shown in Fig. 5.19b. When an SEM image is created, it is critical for the user to understand the relative position of the detector in the scanned image, as given by the azimuthal angle, since the illumination of the image will apparently come from the detector. Note that the "scan rotation" function, which permits the user to arbitrarily choose the angular orientation for the presentation of the image on the display, also varies the apparent angular location of the detector. It is therefore critical for the user to establish what setting of scan rotation corresponds to the correct known value of the detector azimuthal angle.

Good Practice

Make a drawing (top view and side view) of the SEM chamber showing the physical locations of all detectors (electron, X-ray, and cathodoluminescence) and mark the values of the elevation angle, ψ, and azimuthal angle, ζ.

Solid Angle, Ω

As shown in Fig. 5.20, the effective size of the detector with an active area A placed at a distance r from the beam impact point on the specimen is given by the solid angle, Ω (Greek omega, upper case), which is defined as

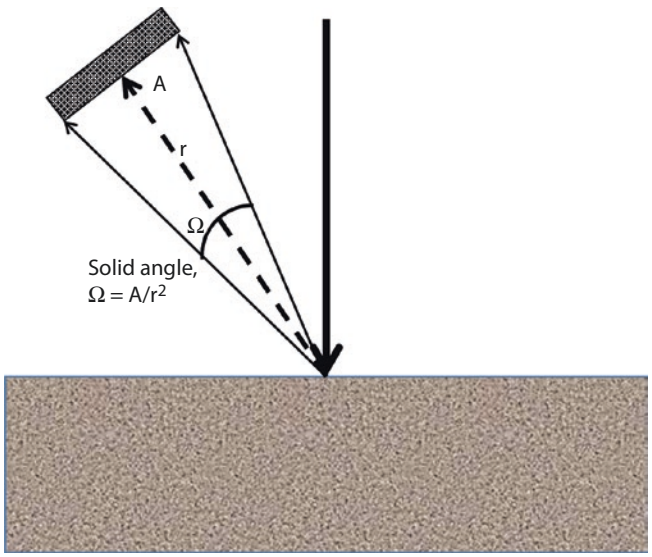

Fig. 5.20 Detector solid angle, Ω

$$\Omega = A / r^2 \ \left(\text{steradians, sr}\right) \tag{5.13}$$

Note the strong dependence of Ω upon the distance of the detector from the beam impact on the specimen.

As an estimate of the overall geometric efficiency, ε, the solid angle of the detector can be compared to the solid angle of the hemisphere (2π sr) into which all electrons leaving a thick target are emitted:

$$\varepsilon = \Omega / 2\pi \tag{5.14}$$

ε provides only an estimate of efficiency because the simple definition in Eq. (5.14) does not consider the non-uniform distribution in the emission of electrons from the specimen, for example, the cosine distribution of BSE at normal incidence.

Energy Response

The response of a detector may be sensitive to the kinetic energy of the striking electron. Generally an electron detector exhibits an energy threshold below which it has no response, usually a consequence of an insensitive surface layer such as a metallic coating, needed to dissipate charging, through which the incident electron must penetrate. Above this threshold, the detector response typically increases with increasing electron energy, making the detector output signal more sensitive to the high energy fraction of the electrons.

Bandwidth

The act of creating an SEM image involves scanning the beam in a time-serial fashion to dwell at a series of discrete beam locations (pixels) on the specimen, with the detector measuring the signal of interest at each location. The signal stream can thus be thought of as changing with a maximum spatial frequency defined by the speed within which successive pixels are sampled. "Bandwidth" is a general term used to describe the range from the lowest to the maximum spatial frequency that can be measured and transmitted through the amplification system. To achieve sufficiently fast scanned imaging to create the illusion of a continuous image ("flicker free") to a human observer, the imaging system must be capable of producing approximately 30 distinct image frames per second.

Ideally, the measurements of successive pixel locations are independent, with the detector returning to its quiescent state before measuring the next pixel. In reality, detectors typically require a finite decay time to dissipate the electron charge accumulated before measuring the next pixel. Thus, as the scanning speed increases so that the time separation of the pixel samples decreases, a limit will eventually be reached where the detector retains a sufficiently high fraction of the signal from the previous pixel so as to interfere with the useful measurement of the signal at the next pixel, producing a visible degradation of the image. When this situation occurs, the detector acts as a bandwidth-limiting device. For the discussion of detector performance characteristics below, detector bandwidth will be broadly classified as "high" (e.g., capable of achieving flicker-free imaging) or "low" (slow scan speeds required).

5.4.3 Common Types of Electron Detectors

Backscattered Electrons

Passive Detectors

Because a large fraction of the BSE emitted from the specimen under conventional operating conditions ($E_0 > 5$ keV) retain 50 % or more of the incident energy, they can be detected with a passive detector that does not apply any post-specimen acceleration to the BSE. Passive detectors include scintillation-based detectors and semiconductor charge-deposition based detectors.

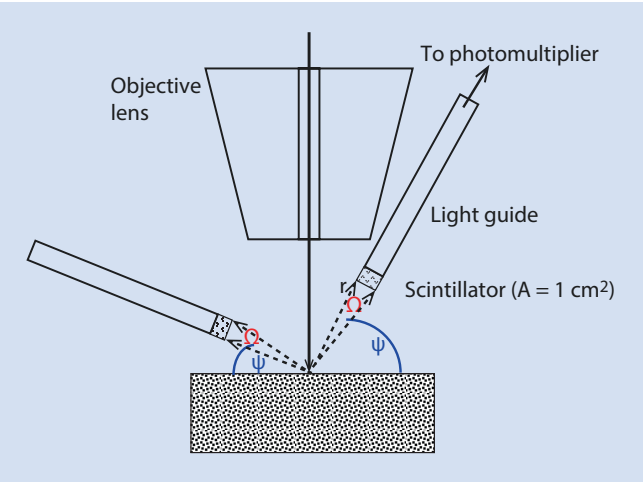

Fig. 5.21 Passive scintillator detectors for BSE. High take-off angle configuration and low take-off angle configuration

Scintillation Detectors

Energetic electrons that strike certain optically active materials cause the emission of light. Optical materials are selected that produce a high signal response that decays very rapidly, thus enabling high bandwidth operation. The emitted light is collected and passed by total internal reflection through a light guide to a photomultiplier, where the light is converted into an electrical signal with very high gain and very rapid time decay, thus preserving the high bandwidth of the original detector signal. Depending on the design, scintillator detectors can vary widely in solid angle. Figure 5.21 shows a small solid-angle design consisting of a small area scintillator (e.g., $A = 1$ cm^2) on the tip of a light guide placed at a distance of 4 cm from the beam impact, giving a solid angle of $\Omega = 0.0625$ sr and a geometric efficiency of $\varepsilon = 0.01$ or 1 %. Both a high take-off angle and a low take-off angle arrangement are illustrated.

Adjustable Controls

Passive BSE detectors on rigid light guides have no user-adjustable operating parameters. (In operation, the "brightness" and "contrast" parameters match the amplified signal from the detector photomultiplier to the acceptable input range of the digitizer.) A passive BSE detector that employs a flexible light guide enables the microscopist to change the take-off angle, azimuthal angle, and the solid angle.

Very large solid angle scintillator-BSE detectors are possible. An example of a large solid angle design is shown in Fig. 5.22 that almost entirely surrounds the specimen with an aperture to permit the access of the beam. For a planar sample set normal to the beam, this detector spans a large range of take-off angles. The scintillator also serves as the light guide, so that a BSE that strikes anywhere on the detector surface can be detected. Due to its large area and close proximity to the specimen, the solid angle approaches 2π sr in size with a geometric efficiency greater than 90 % (Wells 1957; Robinson 1975).

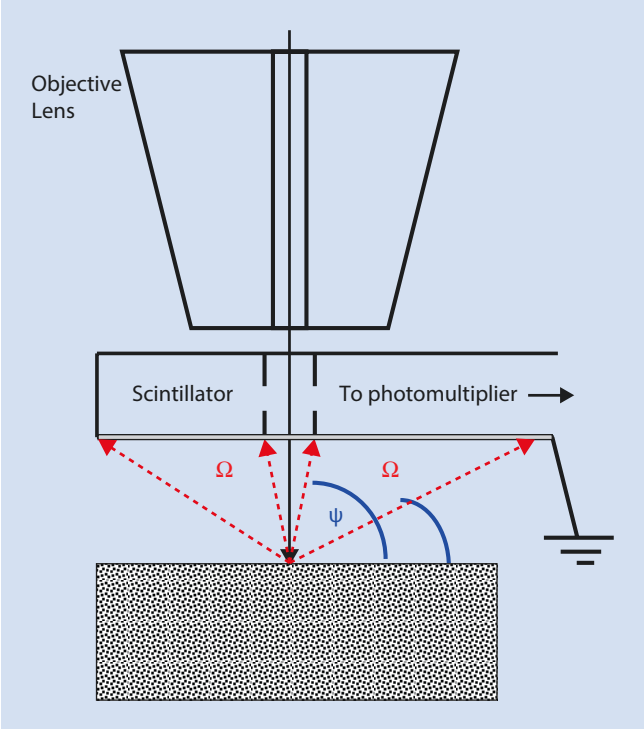

Fig. 5.22 Large solid-angle passive BSE detector

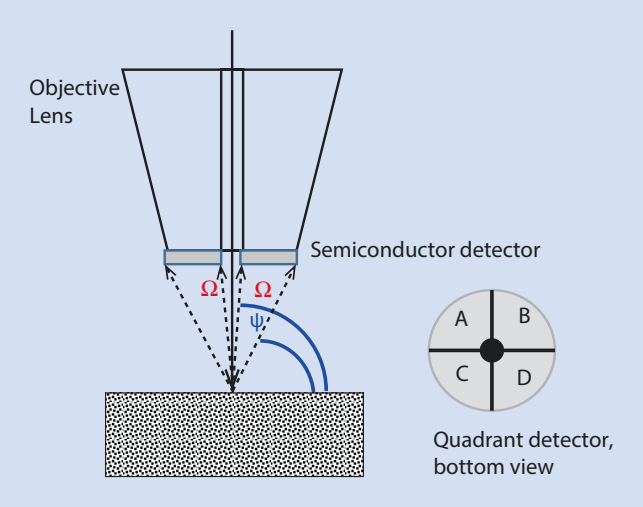

Fig. 5.23 Semiconductor annular detector, quadrant design with four separately selectable sections

Adjustable Controls

The Wells–Robinson scintillation BSE detector is often mounted on an externally controlled, motorized retractable arm. In typical use the detector would be fully inserted to maximize the solid angle. A partial insertion that does not interrupt the beam access to the specimen can be used to intentionally provide an asymmetric detector placement to give an apparent illumination from one side.

Semiconductor BSE Detectors

Certain semiconductor devices can detect energetic electrons that penetrate into the active region of the device where they undergo inelastic scattering. One product of this energy deposition in the semiconductor is the promotion of loosely bound valence shell electrons (each leaving behind a vacancy or positively-charged "hole") into the empty conduction band where they can freely move through the semiconductor in response to an applied potential bias. By applying a suitable electrical field, these free electrons can be collected at a surface electrode and measured. For silicon, this process requires 3.6 eV of energy loss per free electron generated, so that a 15-keV BSE will generate about 4000 free electrons. Thus a BSE current of 1 nA entering the detector will create a collected current of about 4 μA as input for the next amplification stage. The collection electrodes are located on the entrance and back surfaces of the planar wafer detector, which is shown in a typical mounting as an annular detector in Fig. 5.23. The semiconductor BSE detector has the advantage of being thin, so that it can be readily mounted under the objective lens where it will not interfere with other detectors. The size and proximity to the specimen provide a large solid angle and a high take-off angle. As shown in Fig. 5.23, the semiconductor detector can also be assembled from segments, each of which can be used as a separate detector that provides a selectable apparent illumination of the SEM image, or the signals from any combination of the detectors can be added. Semiconductor detectors can also be placed at various locations around the specimen, similar to the arrangement shown for scintillator detectors in Fig. 5.21.

The semiconductor BSE detector has an energy threshold typically in the range 1 keV to 3 keV because of energy loss suffered by the BSE during penetration through the entrance surface electrode. Above this threshold, the response of the detector increases linearly with increasing electron energy, thus providing a greater gain from the high energy fraction of BSE.

Adjustable Controls

The semiconductor BSE detector does not have any user-adjustable parameters, with the exception of the choice of the individual components of a composite multi-detector. In some systems, the individual quadrants or halves can be selected in various combinations, or the sum of all detectors can be used. Some SEMs add an additional semiconductor detector that is placed asymmetrically away from the electron beam to enhance the effect of apparent oblique illumination.

5.4.4 Secondary Electron Detectors

Everhart–Thornley Detector

The most commonly used SEM detector is the Everhart–Thornley (E–T) detector, almost universally referred to as the "secondary electron detector." Everhart and Thornley

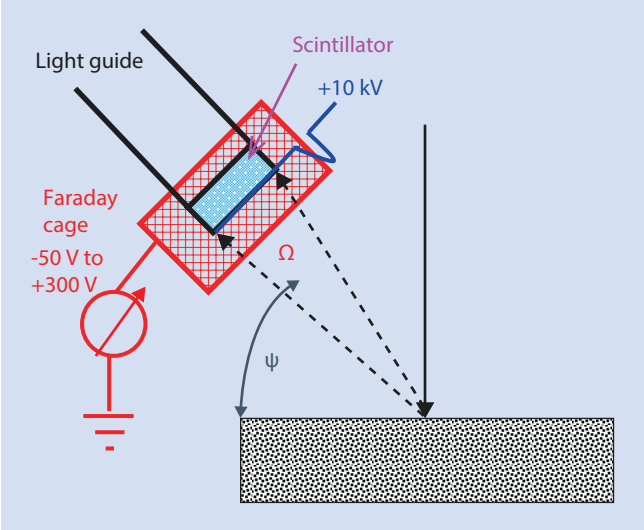

Fig. 5.24 Schematic of Everhart–Thornley detector showing the scintillator with a thin metallic surface electrode (*blue*) with an applied bias of positive 10 kV surrounded by an electrically isolated Faraday cage (*red)* which has a separate bias supply variable from negative 50 V to positive 300 V

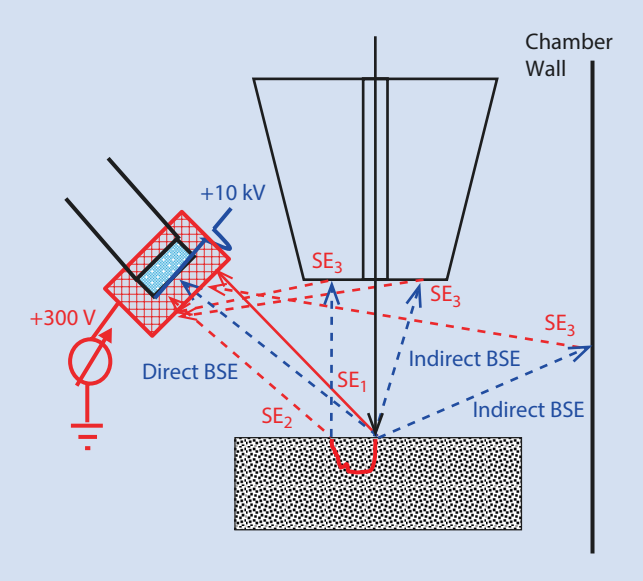

Fig. 5.25 Schematic of electron collection with a +300 V Faraday cage potential. Signals collected: direct BSE that enter solid angle of the scintillator; SE_1 produced within beam entrance footprint; SE_2 produced where BSE emerge from specimen; SE_3 produced where BSE strike the pole piece and chamber walls. SE_2 and SE_3 collection actually represents the remote BSE that could otherwise be lost

(1957) solved the problem of detecting very low energy secondary electrons by using a scintillator with a thin metal coating to which a large positive potential, 10 kV or higher, is applied. This post-specimen acceleration of the secondary electrons raises their kinetic energy to a sufficient level to cause scintillation in an appropriate material (typically plastic or glass doped with an optically active compound) after penetrating through the thin metallization layer that is applied to discharge the insulating scintillator. To protect the primary electron beam from any degradation due to encountering this large positive potential asymmetrically placed in the specimen chamber, the scintillator is surrounded by an electrically isolated "Faraday cage" to which is applied a modest positive potential of a few hundred volts (in some SEMs, the option exists to select the bias over a range typically from −50 to + 300 V), as shown in Fig. 5.24. The primary beam is negligibly affected by exposure to this much lower potential, but the secondary electrons can still be collected with great efficiency to the vicinity of the Faraday cage, where they are then accelerated by the much higher positive potential applied to the scintillator.

While the E–T detector does indeed detect the secondary electrons emitted by the sample, the nature of the total collected signal is actually quite complicated because of the different sources of secondary electrons, as illustrated in Fig. 5.25. The SE_1 component generated within the landing footprint of the primary beam on the specimen cannot be distinguished from the SE_2 component produced by the exiting BSE since they are produced spatially within nanometers to micrometers and they have the same energy and angular distributions. Since the SE_2 production depends on the BSE, rising and falling with the local effects on backscattering, the SE_2 signal actually carries BSE information. Moreover, the BSE are sufficiently energetic that while they are not significantly deflected and collected by the low Faraday cage potential, the BSE continue along their emission trajectory until they encounter the objective lens pole piece, stage components, or sample chamber walls, where they generate still more secondary electrons, designated SE_3. Although SE_3 are generated centimeters away from the beam impact, they are collected with high efficiency by the Faraday cage potential, again constituting a signal carrying BSE information since their number depends on the number of BSE ("indirect BSE"). Finally, those BSE emitted by the specimen into the solid angle defined by the E-T scintillator disk are detected ("direct BSE"). This complex mixture of signals plays an important role in creating the apparent illumination of the "secondary electron image."

Adjustable Controls

On some SEMs the Faraday cage bias of the Everhart–Thornley detector can be adjusted, typically over a range from a negative potential of –100 V or less to a positive potential of a few hundred volts. When the Faraday cage potential is set to zero or a few volts negative, secondary electron collection is almost entirely suppressed, so that only the direct BSE are collected, giving a scintillator BSE detector that is of relatively small solid angle and asymmetrically placed on one side of the specimen. When the Faraday cage potential is set to the maximum positive value available, the

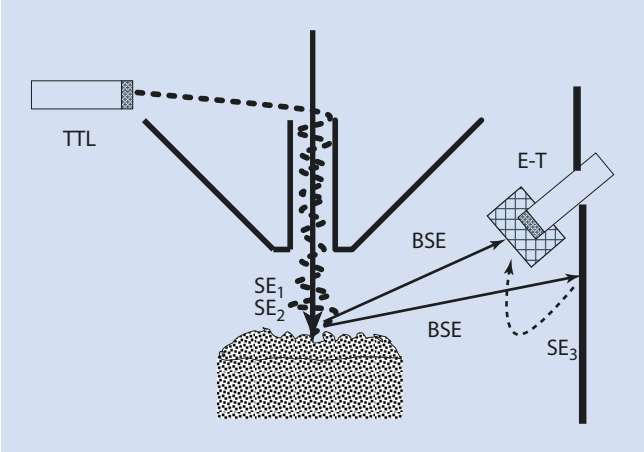

Fig. 5.26 "Through-the-lens" (TTL) secondary electron detector

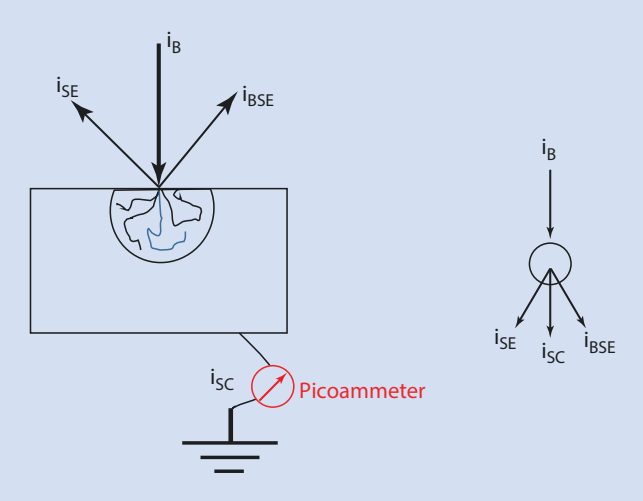

Fig. 5.27 Currents flowing in and out of the specimen and the electrical junction equivalent

complete suite of SE_1, SE_2, SE_3, and the direct BSE is collected, creating a complex mix of BSE and true SE image contrast effects.

Through-the-Lens (TTL) Electron Detectors

TTL SE Detector

In SEMs where the magnetic field of the objective lens projects into the specimen chamber, a "through-the-lens" (TTL) secondary electron detector can be implemented, as illustrated schematically in Fig. 5.26. SE_1 from the incident beam footprint and SE_2 emitted within the BSE surface distribution are captured by the magnetic field and spiral up through the lens. After emerging from the top of the lens, the secondary electrons are then attracted to an Everhart–Thornley type biased scintillator detector. The advantage of the TTL SE detector is the near complete exclusion of direct BSE and the abundant SE_3 class generated by BSE striking the chamber walls and pole piece. Since these remote SE_3 are generated on surfaces far from the optic axis of the SEM, they are not efficiently captured by the lens field. Because the SE_3 class actually represents low resolution BSE information, removing SE_3 from the overall SE signal actually improves the sensitivity of the image to the true SE_1 component, which is still diluted by the BSE-related SE_2 component. A further refinement of the through-the-lens detector is the introduction of energy filtering which allows the microscopist to select a band of SE kinetic energy.

TTL BSE Detector

For a flat specimen oriented normal to the beam, the cosine distribution of BSE creates a significant flux of BSE that pass up through the bore of the objective lens. A TTL BSE detector is created by providing either a direct scintillation BSE detector or a separate surface above the lens for BSE-to-SE conversion and subsequent detection with another E-T type detector.

5.4.5 Specimen Current: The Specimen as Its Own Detector

The Specimen Can Serve as a Perfect Detector for the Total Number of BSE and SE Emitted

Consider the interaction of the beam electrons to produce BSE and SE. For a 20-keV beam incident on copper, about 30 out of 100 beam electrons are backscattered ($\eta = 0.3$). The remaining 70 beam electrons lose all their energy in the solid, are reduced to thermal energies, and are captured. Additionally, about 10 units of charge are ejected from copper as secondary electrons ($\delta = 0.1$). This leaves a total of 60 excess electrons in the target. What is the fate of these electrons? To understand this, an alternative view is to consider the electron currents, defined as charge per unit time, which flow in and out of the specimen. Viewed in this fashion, the specimen can be treated as an electrical junction, as illustrated schematically in Fig. 5.27, and is subject to the fundamental rules which govern junctions in circuits. By Thevinin's junction theorem, the currents flowing in and out of the junction must exactly balance, or else there will be net accumulation or loss of electrical charge, and the specimen will charge on a macroscopic scale. If the specimen is a conductor or semiconductor and if there is a path to ground from the specimen, then electrical neutrality will be maintained by the flow of a current, designated the "specimen current" (also referred to as the "target current" or "absorbed current"), either to or from ground, depending on the exact conditions of beam energy and specimen composition. What is the magnitude of the specimen current?

Considering the specimen as a junction, the current flowing into the junction is the beam current, i_B, and the currents flowing out of the junction are the backscattered electron current, i_{BS}, and the secondary electron current, i_{SE}. For charge balance to occur, the specimen current, i_{SC}, is given by

$$i_{SC} = i_B - i_{BS} - i_{SC} \quad (5.15)$$

For the copper target, the BSE current will be $i_{BSE} = \eta \times i_B = 0.3\ i_B$ and the SE current will be $i_{SE} = \delta \times i_B = 0.1\ i_B$. Substituting these values in Eq. (5.15) gives the result that the specimen current will be $i_{SC} = 0.6\ i_B$, double the largest of the conventional emitted imaging currents, the BSE signal. If a path to ground is not provided so that the specimen current can flow, the specimen will rapidly charge.

Note that in formulating Eq. (5.15) no consideration is given to the large difference in energy carried by the BSE and SE. Since current is the passage of charge per unit time, the ejection of a 1 eV SE from the specimen carries the same weight as a 10 keV BSE in affecting the specimen current signal. Moreover, the specimen current is not sensitive to the direction of emission of BSE and SE, or to their subsequent fate in the SEM specimen chamber, as long as they do not return to the specimen as a result of re-scattering. Thus, specimen current constitutes a signal that is sensitive only to number effects, that is, the total numbers of BSE and SE leaving the specimen.

The specimen serves as its own collector for the specimen current. As such, the specimen current signal is readily available just by insulating the specimen from electrical ground and then measuring the specimen current flowing to ground through a wire to ground. Knowledge of the actual specimen current is extremely useful for establishing consistent operating conditions, and is critical for dose-based X-ray microanalysis. The original beam current itself be measured by creating a "Faraday cup" in the specimen or specimen stage by drilling a blind hole and directing the incident beam into the hole: since no BSE or SE can escape the Faraday cup, the measured specimen current then must equal the beam current. But by measuring the specimen current as a function of the beam position during the scan, an image can be formed that is sensitive to the total emission of BSE and SE regardless of the direction of emission and their subsequent fate interacting with external detectors, the final lens pole piece, and the walls of the specimen chamber. Does the specimen current signal actually convey useful information? As described below under contrast formation, the specimen current signal contains exactly the same information as that carried by the BSE and SE currents. Since external electron detectors measure a convolution of backscattered and/or secondary current with other characteristics such as energy and/or directionality, the specimen current signal can give a unique view of the specimen (Newbury 1976).

To make use of the specimen current signal, the current must be routed through an amplifier on its way to ground. The difficulty is that we must be able to work with a current similar in magnitude to the beam current, without any high gain physical amplification process such as electron-hole pair production in a solid state detector or the electron cascade in an electron multiplier. To achieve acceptable bandwidth at the high gains necessary, most current amplifiers take the form of a low input impedance operational amplifier (Fiori et al. 1974). Such amplifiers can operate with currents as low as 10 pA and still provide adequate bandwidth to view acceptable images at slow visual scan rates (one 500-line frame/s).

5.4.6 A Useful, Practical Measure of a Detector: Detective Quantum Efficiency

The geometric efficiency is just one factor in the overall performance of a detector, and while this quantity is relatively straightforward to define in the case of a passive BSE detector, as shown in Fig. 5.20, it is much more difficult to describe for an E–T detector because of the mix of BSE and direct SE_1 and SE_2 signal components and the complex conversion and collection of the remote SE_3 component produced where BSE strike the objective lens, BSE detector, and chamber walls. A second important factor in detector performance is the efficiency with which each collected electron is converted into useful signal. Thirdly, noise may be introduced at various stages in the amplification process to the digitization which creates the final intensity recorded in the computer memory for the pixel at which the beam dwells.

All of these factors are taken into account by the detective quantum efficiency (DQE). The DQE is a robust measure of detector performance that can be used in the calculation of limitations imposed on imaging through the threshold current/contrast equation (Joy et al. 1996).

The DQE is defined as (Jones 1959)

$$\mathrm{DQE} = \left(S/N\right)^2_{\text{experimental}} / \left(S/N\right)^2_{\text{theoretictal}} \quad (5.16)$$

where S is the signal and N is the noise. Determining the DQE for a detector requires measurement of the experimental S/N ratio as produced under defined conditions of specimen composition, beam current and pixel dwell time that enable an estimate of the corresponding theoretical S/N ratio. This measurement can be performed by imaging a featureless specimen that ideally produces a fixed signal response which translates into a single gray level in the digitally recorded image, giving a direct measure of the signal, S. The corresponding noise, N, is determined from the measured width of the distribution of gray levels around the average value.

Measuring the DQE: BSE Semiconductor Detector

Joy et al. (1996) describe a procedure by which the experimental S/N ratio can be estimated from a digital image of a specimen that produces a unique gray level, so that the broadening observed in the image histogram of the ideal gray level is a quantitative measure of the various noise sources that are inevitable in the total measurement process that produces the image. Thus, the first requirement is a specimen with a highly polished featureless surface that will produce unique values of η and δ and which does not contribute any other sources of

contrast (e.g., topography, compositional differences, electron channeling, or most problematically, changing δ and η values due to the accumulation of contamination). A polished silicon wafer provides a suitable sample, and with careful precleaning, including plasma cleaning in the SEM airlock if available, the contamination problem can be minimized satisfactorily during the sequence of measurements required. As an alternative to silicon, a metallographically polished (but not etched) pure metallic element (metallic) surface, such as nickel, molybdenum, gold, etc., will be suitable. Because calculation of the theoretical S/N ratio is required for the DQE calculation with Eq. 5.16, the beam current must be accurately measured. The SEM must thus be equipped with a picoammeter to measure the beam current, and if an in-column Faraday cup is not available, then a specimen stage Faraday cup (e.g., a blind hole covered with a small [e.g., <100-μm-diameter] aperture) is required to completely capture the beam without loss of BSE or SE so that a measurement of the specimen current equals the beam current.

Because the detector will have a "dark current," i.e., a response with no beam current, it is necessary to make a series of measurements with changing beam current. It is also important to defeat any automatic image gain scaling that some SEMs provide as a "convenience" feature for the user that acts to automatically compensate for changes in the incident beam current by adjusting the imaging amplifier gain to maintain a steady mid-range gray level.

Measurement sequence

1. Choose a beam current which will serve as the high end of the beam current range, and using the image histogram function, adjust the imaging amplifier controls (often designated "contrast" and "brightness") to place the average gray level of the specimen near the top of the range, being careful that the upper tail of the gray level distribution of the image of the specimen does not saturate ("clip") at the maximum gray level (255 for an 8-bit image, 65,535 for a 16-bit image).
2. Keeping the same values for the image amplifier parameters (autoscaling of the imaging amplifier must be defeated before beginning the measurement process), choose a beam current that places the average gray level of the specimen near low end of the gray level range, checking to see that the gray level distribution of the image is completely within the histogram range—that is, there is no clipping of the distribution at the bottom (black) of the range.
3. With the minimum and maximum of the current range established, record a sequence of images with different beam currents between the low and high values and use the image histogram tool to determine the average gray level for each beam current.
4. A graphical plot of data measured with a semiconductor BSE detector for a polished Mo target produces the result illustrated in Fig. 5.28, where the y-axis intercept value is a measure of the dark current gray level intensity, GL_{DC} (corresponding to zero beam current) of this particular BSE detector.

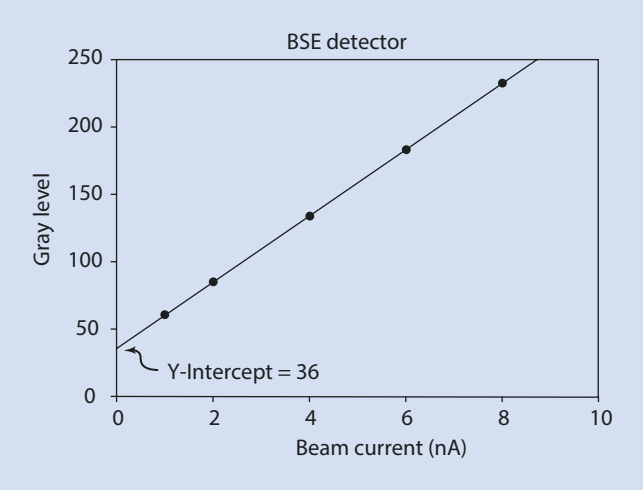

Fig. 5.28 Plot of measured gray level versus incident beam current for a BSE detector. $E_0 = 20$ keV; Mo target

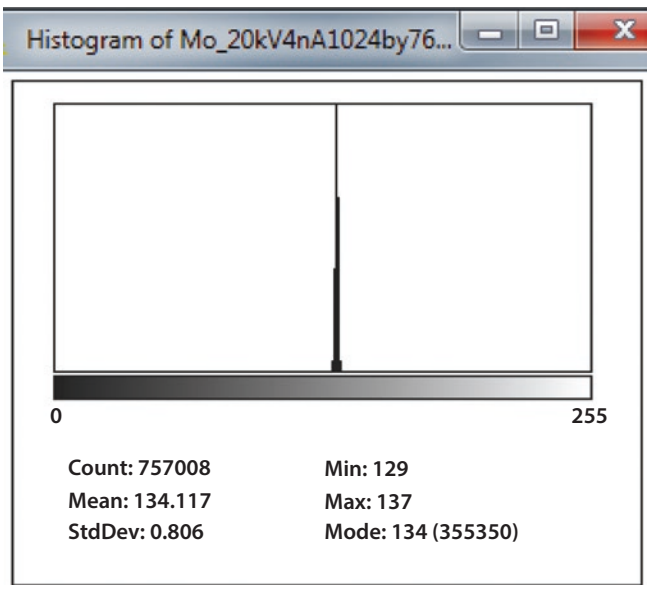

Fig. 5.29 Output of image histogram from IMAGE-J for the 4 nA image from Fig. 5.28

5. Choose an image recorded within this range and determine the mean gray level, G_{mean}, and the variance, S_{var} (the square of the standard deviation) using the image histogram function, as shown in Fig. 5.29.

Calculation sequence:

$$(S/N)_{experimental} = (GL_{mean} - GL_{DC})/S_{var} \quad (5.17)$$

where is S_{var} the variance (the square of the standard deviation) of the gray level distribution. For the values in Fig. 5.29 for the 4 nA data point obtained with ImageJ-Fiji,

$$(S/N)_{experimental} = (134.3 - 36)/0.575^2 = 297.3 \quad (5.18)$$

The corresponding theoretical S/N ratio is estimated from the number n of BSE produced, which depends on the incident beam current I_B, the BSE coefficient η, and the dwell time per pixel τ:

$$n = 6.24\, I_B\, \eta\, \tau \tag{5.19}$$

where the coefficient 6.24 is appropriate for beam current expressed in pA and the dwell time expressed in µs.

Because the image pixels are independent and uncorrelated, if a mean number n of BSE is produced at each pixel the expected variance is $n^{1/2}$:

$$(S/N)_{\text{theory}} = n/n^{1/2} = n^{1/2} = (6.24\, I_B\, \eta\, \tau)^{1/2} \tag{5.20}$$

For $I_B = 4000$ pA, $\eta_{Mo} = 0.38$, and $\tau = 64$ µs

$$(S/N)_{\text{theory}} = (6.24\, I_B\, \eta\, \tau)^{1/2} = 779.1 \tag{5.21}$$

The DQE for this particular detector is thus

$$\begin{aligned} \text{DQE} &= (S/N)^2_{\text{experimental}} / (S/N)^2_{\text{theoretictal}} \\ &= 297.3^2 / 779.1^2 = 0.146 \end{aligned} \tag{5.22}$$

A similar study for an Everhart–Thornley SE-BSE detector on an electron probe X-ray microanalyzer is shown in Fig. 5.30, for which the DQE is calculated as 0.0016. Table 5.1 lists values of the DQE for various detectors, demonstrating that a large range in values is encountered, even among detectors of a specific class, for example, the E–T detector.

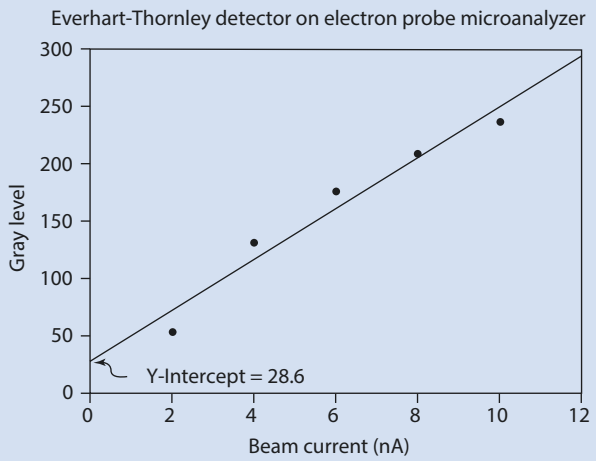

Fig. 5.30 Average gray level versus beam current for an Everhart–Thornley detector on an electron probe microanalyzer. Specimen: Si; $E_0 = 10$ keV

Table 5.1 DQE of electron detectors from different manufacturers (Joy et al. 1996)

SE detector	DQE
Everhart–Thornley	0.56
Everhart–Thornley	0.17
Everhart–Thornley	0.12
Everhart–Thornley	0.017
Everhart–Thornley	0.0008
High performance SEM:	
Everhart–Thornley (lower)	0.18
Everhart–Thornley (TTL)	0.76
Microchannel plate	0.029
BSE detector	
Scintillator BSE	0.043
Scintillator BSE	0.005
E–T BSE mode (negative bias)	0.001
E–T BSE mode (negative bias)	0.004
Microchannel plate BSE	0.058
Microchannel plate BSE	0.026

References

Everhart T, Thornley R (1960) Wide-band detector for micro-microampere low-energy electron currents. J Sci Instrum 37:246

Fiori C, Yakowitz H, Newbury D (1974) Some techniques of signal processing in scanning electron microscopy. In: Johari O (ed) SEM/1974. IIT Research Institute, Chicago, p 167

Jones R (1959) Phenomenological description of the response and detecting ability of radiation detectors. Adv Electr Electron Opt 11:88

Joy DC, Joy CS, Bunn RD (1996) Measuring the performance of scanning electron microscope detectors. Scanning 18:533

Newbury DE (1976) "The utility of specimen current imaging in the scanning electron microscope" SEM/1976/I. IIT Research Inst, Chicago, p 111

Robinson V (1975) "Backscattered electron imaging" SEM/1975, I. IIT Research Inst, Chicago, p 51

Wells OC (1957) The construction of a scanning electron microscope and its application to the study of fibres. Ph. D. Diss., Cambridge University, Cambridge